# Journal Pre-proof

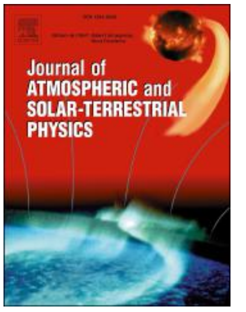


Evaluation of telluric-associated corrosion on buried pipelines

L. Trichtchenko, A.P. Trishchenko, P. Hejda, R. Langer

PII: S1364-6826(23)00080-9

DOI: https://doi.org/10.1016/j.jastp.2023.106082

Reference: ATP 106082

To appear in: *Journal of Atmospheric and Solar-Terrestrial Physics*

Received Date: 26 July 2022

Revised Date: 5 April 2023

Accepted Date: 16 May 2023

# Evaluation of telluric-associated corrosion on buried pipelines

**L.Trichtchenko[1], A.P. Trishchenko[1], P. Hejda[2], R Langer[1]**

[1]Natural Resources Canada, Ottawa, Canada

[2]Institute of Geophysics, Czech Academy of Sciences, Prague, Czech Republic

Corresponding author: Larisa Trichtchenko

Email: larisa.trichtchenko@gmail.com

Keywords: space weather, geomagnetically induced currents, telluric currents, corrosion

**Abstract**

Telluric currents, often known as geomagnetically induced currents (GIC), are produced by the natural variations of the Earth's magnetic field.

The corrosion protection system of a buried pipeline generally comprises the coating and cathodic protection system. Cathodic protection is an electrochemical protection system that maintains the pipe-to-soil potential (PSP) sufficiently negative in order to reduce corrosion to negligible levels. Varying telluric currents alter the PSP, thus interfering with the pipeline corrosion protection system and can create conditions when corrosion might increase above acceptable levels.

This paper presents an evaluation of telluric-associated corrosion derived from measured and modelled PSP variations. The corrosion rates (metal loss per year) due to varying telluric currents with continuous frequency spectra (1 Hz to $10^{-5}$ Hz) are approximated with the use of published experimental results derived for the specific sets of fixed frequencies.

Results are presented for PSP observed on Australian and European pipelines during two periods of strong geomagnetic activity (in 2003 and 2004) and for identical hypothetical pipelines located at different latitudes for the entire year 2004.

From the analysis of recorded PSP, it was found that the corrosion rates for a near-equatorial pipeline (Australia) could be higher than for mid-latitudes (Europe). This is possible because telluric-associated corrosion rates depend not only on geomagnetic activity, but on the properties of the pipeline coating, the performance of the cathodic protection system and environmental conditions. The study demonstrated that without cathodic protection the estimated corrosion rates exceeded the benchmark values recommended by national and international standards, and in exceptional case can exceed the acceptable values even with cathodic protection.

Telluric-associated corrosion estimated for the identical hypothetical pipelines located in zones with different geomagnetic activity, clearly demonstrated the latitudinal dependence. The substantial increase of corrosion rates (about 5 times) has been found with increase of latitude from subauroral to auroral locations.

## 1. Introduction

Buried oil and gas transmission pipelines, being made from steel, are subject to corrosion, which is one of the main concerns for their operational safety. Several methods are used to protect pipelines from corrosion (Peabody, 2001). The first line of protection includes the highly resistive durable coating layer. The mechanical and temperature stresses imposed on pipelines require monitoring of the coating and pipeline integrity, a challenging task for buried pipelines which can extend hundreds of kilometers in remote areas. To further enhance the level of protection, the cathodic protection system is commonly used. This system charges and maintains the pipeline steel electrically negative with respect to the surrounding soil (Peabody, 1979; Degerstedt et al., 1995; Peabody, 2001; Gummow, 2001; Revie (ed.), 2015).

For cathodic protection to work effectively, the protection potentials should be maintained within the range of acceptable values, depending on the pipeline characteristics and environmental conditions. Typically, these levels would be between -1.2 V and -0.85 V (e.g., ISO 15589-1, 2015; NACE SP0169, 2013). In accordance with ISO 13623 (2017), the allowable corrosion rate for the pipeline is determined by the pipeline designer. With effective cathodic protection, a corrosion rate of 0.01 mm/ year can be achieved under certain circumstances (ISO 21857, 2021; ISO 15589-1, 2015). In North America, a value of 0.025 mm/year or less is recommended as a benchmark (NACE SP0169, 2013) value for an allowable annual corrosion rate.

Telluric (i.e. “geomagnetically induced”) currents are driven in the Earth and earthed conductors, such as pipelines, by variations of the geo-electromagnetic fields. These varying currents can enter and exit the steel pipeline at places where the coating has defects, thus producing the PSP variations with respect to the recommended CP level. Corrosion can occur when telluric currents are exiting the pipeline at the contact of bare steel with soil (e.g. Campbell, 1978; Martin, 1993; Ingham et al., 2022). An extensive list of references on telluric current interference with pipelines is provided in Boteler and Trichtchenko (2015).

An example of simultaneous measurements of the geomagnetic field variations (at Ottawa Geomagnetic Observatory, Canada), geoelectric field variations (at location in Southern Ontario) and PSP variations at a site on the pipeline in Nova Scotia, Canada, during the geomagnetic storm on 6-7 April 2000 is presented in Fig. 1.

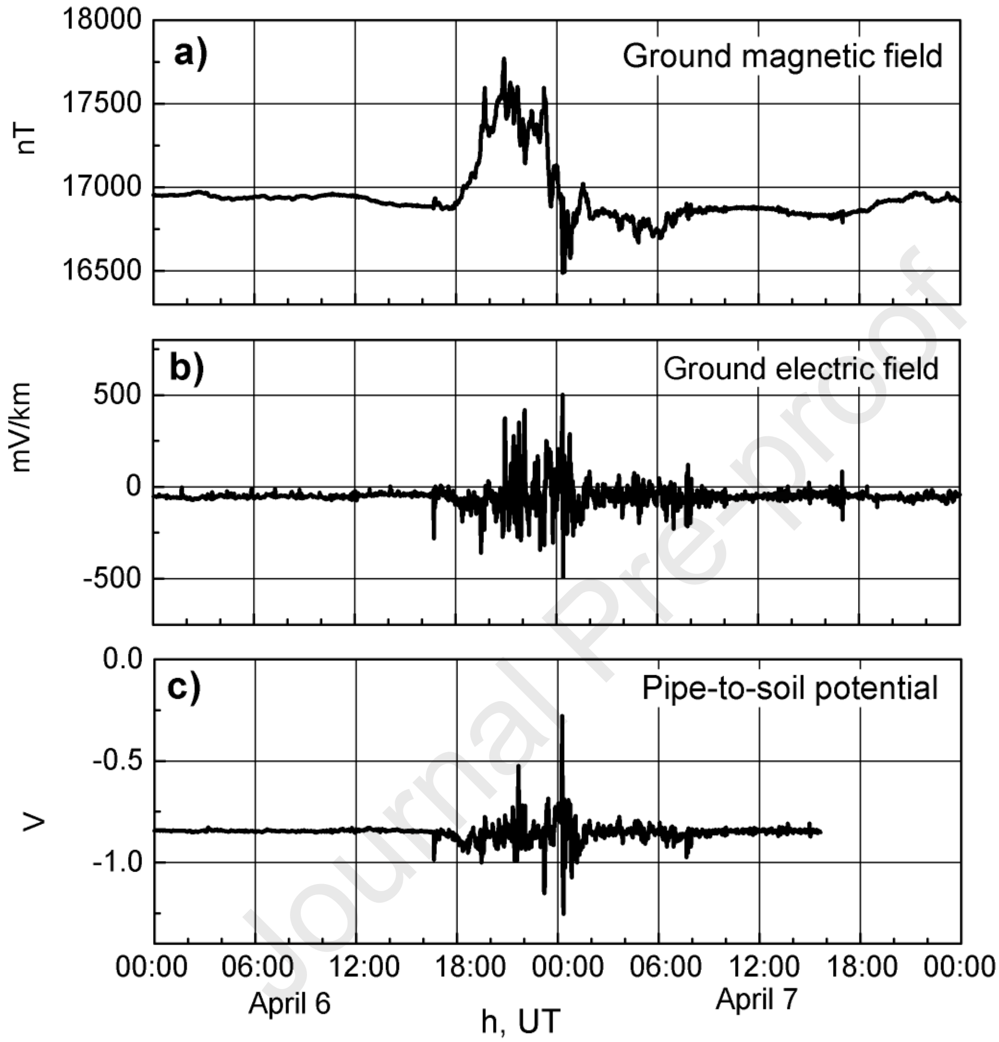


Fig. 1. Measurements performed during geomagnetic storm on April 6-7, 2000, of the following characteristics: a) geomagnetic field at Ottawa Geomagnetic Observatory, b) geoelectric field in Southern Ontario, and c) PSP variations on Maritime pipeline in Nova Scotia.

As can be seen from Fig. 1, the increase in variations of the geomagnetic field during the geomagnetic storm enhances variations in the geoelectric field. This drives larger telluric currents, which, in turn, amplifies the PSP variations.

The intense and prolonged variations of PSP caused by telluric currents introduce inaccuracies in the estimation of the CP levels which are regularly monitored for safety reasons. This type of telluric interference is well known and is addressed in multiple research papers and technical documents (e.g., Degerstedt et al 1995; Place and Sneath, 2001; NACE TM0497, 2018; NACE SP0104, 2020; ISO 21857, 2021). Recently published results by Buchler (2020) presented an approach evaluating telluric-related corrosion risks through extrapolation of theoretical and experimental CP criteria obtained for pipeline interference with a DC-traction system. These results have been also included in the technical guidelines and recommendations of ISO 21857 (2021). However, these publications do not present the estimation of telluric-associated corrosion rates.

Most of the theoretical results and experimental data on pipeline corrosion are concerned with the naturally occurring electrochemical processes caused by constant direct currents (DC). These are well described, for example, in Peabody (2001). Another source of corrosion that attracts a lot of attention is alternating current (AC)-related corrosion caused by the electromagnetic interference from man-made AC-sources, such as power lines, trams, trains, and others (Gummow et al., 1996; Revie (ed.), 2015 and references therein, ISO 15589-1). Corrosion due to the low-frequency telluric currents fluctuating with periods from 1 second to 24 hours has attracted less attention. In earlier works by Gideon et al. (1970) and Campbell (1978), it has been estimated as negligible, although Peabody (1979) stated that the risk of corrosion due to telluric currents should not be ignored, a conclusion that later has been supported by Osella et al. (1999).



A comprehensive approach to the evaluation of pipeline corrosion due to telluric currents was presented in Gummow (2002). The approach was based on the statistical estimation of the cumulative occurrences of geomagnetic disturbances using the 3-hour $K_p$ index of geomagnetic activity, derived PSP variations, and experimental corrosion rate data published by McCollum and Ahlborn (1916). Gummow (2002) concluded that the increased corrosion during periods of high geomagnetic activity with $K_p>5$ could exceed the corrosion rate of 0.025 mm/year level recommended as a benchmark in NACE SP0169, 2013 (and, therefore, a level of 0.010 mm/year recommended in ISO 15589-1, 2015). Following the approach established by Gummow (2002), Ingham and Rodger (2018) estimated the corrosion on the pipeline in New Zealand for similar geomagnetic conditions (i.e. $K_p$>5). Both studies assumed that the telluric current is constant for the 3-hour interval used to derive the $K_p$ index, ignoring the actual variability of telluric currents. Moraes et al. (2020), estimated the telluric-associated corrosion on a pipeline in Brazil for the geomagnetic storm of March 17, 2015, using modelled PSP variations, thus including the variability of the telluric currents. All these studies came to a similar conclusion that telluric-associated corrosion can exceed the maximum acceptable level.

The purpose of the present study is to advance the evaluation of corrosion due to telluric currents. Rather than using geomagnetic indices, the study employs recorded and modelled PSP variations. The reference corrosion data for our study were taken from several sources, including the widely used McCollum and Ahlborn (1916), as well as more recent studies by Birbilis et al. (2005); Qin et al. (2020) and Du et al. (2021).

Fig. 2 outlines two approaches used in our study.

1) Evaluation of corrosion during geomagnetic storms based on available PSP observations. In this case, corrosion models derived from the above-mentioned published sources were applied to the measured PSP values (solid line boxes in Fig. 2).

2). Evaluation of corrosion during the entire year 2004, with several additional steps and models used to calculate the PSP variations (dashed line boxes in Fig. 2). The input data consisted of observations of the geomagnetic field variations, regularly monitored over long periods of time at the geomagnetic observatories.

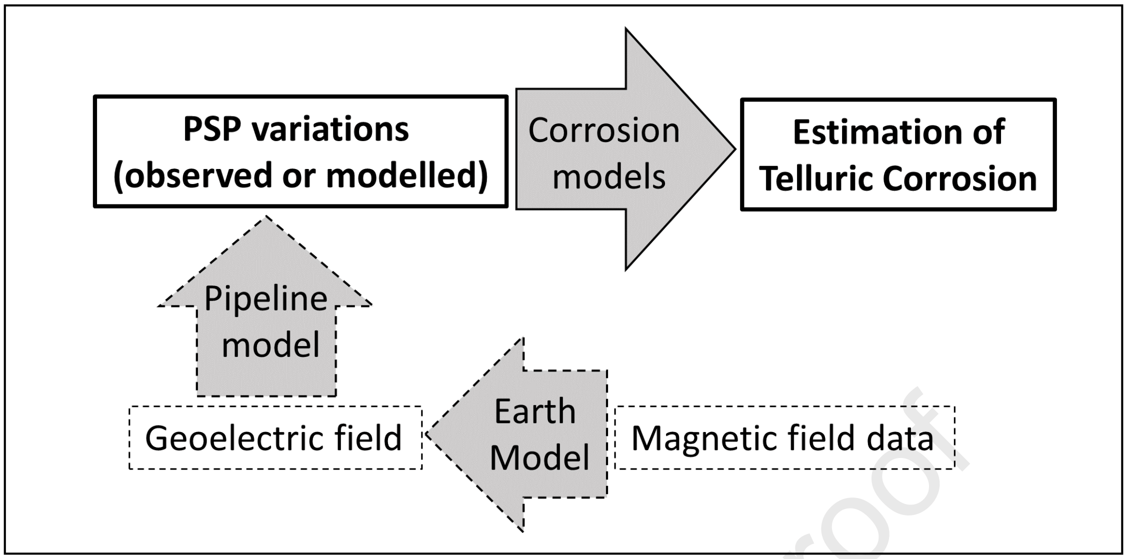


Fig. 2. Logic diagram used for evaluation of the telluric corrosion on pipelines.

The paper is structured as follows:

Section 2 describes the observational data, such as pipeline PSP recordings and geomagnetic measurements. Section 3 outlines the approach for modelling the annual time series of PSP variations, Section 4 presents the details of the corrosion rate datasets compiled from the published sources. Main results are presented in Section 5, followed by Discussion (Section 6) and Summary (Section7).

## 2. Observational data

Continuous monitoring and archiving of pipeline data are not widely implemented, and the recordings of PSP are not readily available for the researchers. They are usually obtained directly from pipeline companies as a part of joint research projects. The policy on data use and dissemination is defined by each company, often with various restrictions. The modelled PSP time series are more frequently used for the assessment of telluric current effects on PSP variations, especially to investigate the impact of different geomagnetic conditions on the same pipeline for design and mitigation purposes.

For the evaluations presented here, both measured and modelled PSP data are used. Observed PSP variations were recorded on the Australian pipeline during November 3-15, 2004 (Trichtchenko et al., 2007), and on two pipelines in Europe during October-November 2003 (Hejda and Bochníček, 2005). The recording sites on the Australian pipeline were located at ~ 20°S latitude and the recording sites on the European pipelines were located at ~ 50°N in the Czech Republic. These two sets of PSP observations provide a unique opportunity to evaluate telluric-associated corrosion caused by space weather based on observations during two of the most significant space weather events in the solar cycle 23.

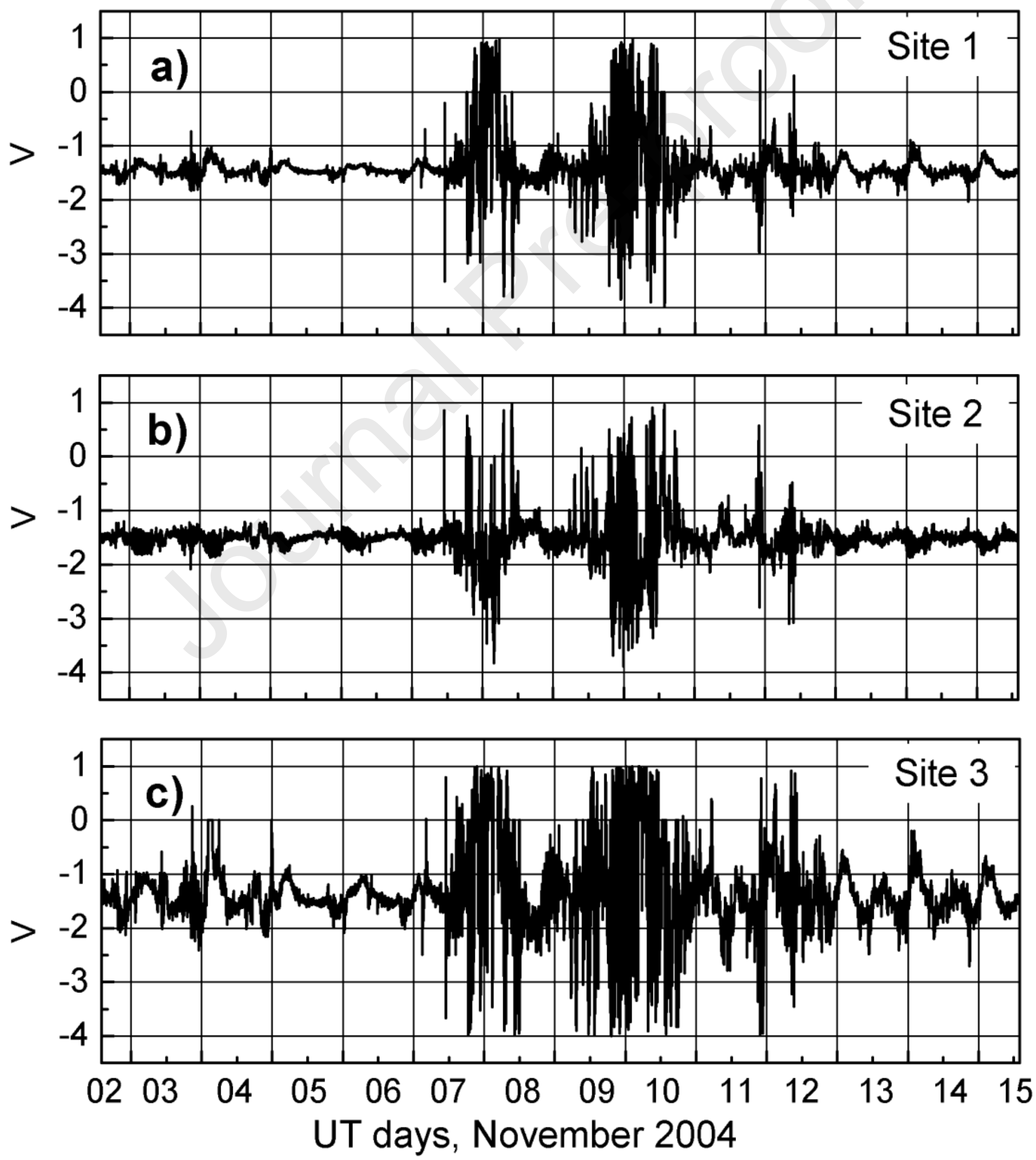

Fig. 3. PSP variations (data with 1 min sampling interval) recorded at 3 sites along the Australian pipeline during 13 days in November 2004, which includes two periods of magnetic storms. Note, that UT days do not coincide with days in Australian local time (UT+10 hours), thus the start and the end of observations do not coincide with UT days.

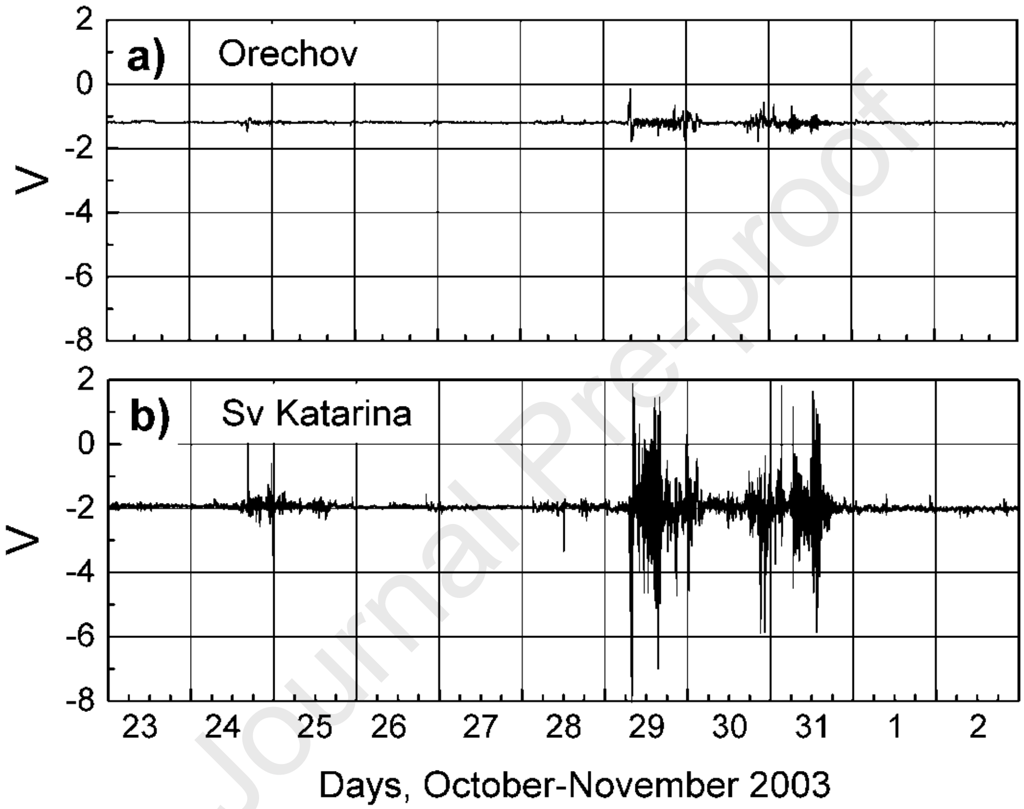


Fig. 4. PSP variations (30 s sampling interval) recorded during October 23-November 2, 2003, space weather events on two European pipelines, Druzba and Ingolstadt–Kralupy–Litvínov (IKL) at sites located in the Czech Republic: a) Orechov (Druzba) and b) Sv Katarina (IKL).

Figs. 3 and 4 present the observed variations of PSP on Australian and European pipelines. During the November 2004 event (Fig. 3), the PSP variations on a pipeline at the equatorial location in Australia were larger than recorded at Orechov (Fig. 4a) on the Druzba pipeline at a higher latitude (~50°N) during the similar geomagnetic storms of October-November 2003 event. The PSP variations, recorded at Sv Katarina (IKL pipeline), were much larger than the ones observed at

Orechov (Fig. 4) for the same event. These differences can be attributed to the different electrical characteristics of the coating on two pipelines (see Hejda and Bochníček, 2005, for more details).

Comparisons of PSP variations due to telluric currents on different pipelines might give inconsistent results due to external factors, such as in the local geomagnetic variations, and due to the pipeline characteristics (i.e. pipeline steel, coating, topology, corrosion protection system, etc.).

To assess the telluric-associated corrosion on the same pipeline at a wider range of latitudes, the PSP variations were modelled based on the 5 s data available from three Canadian Geomagnetic Observatories: Fort Churchill (FCC, 58.8° N, 265.9°E) Meanook (MEA, 54.6°N, 246.6°E) and Ottawa (OTT, 45.4°N, 284.4°E) for the entire year 2004.
The selected year includes two periods of strong geomagnetic activity, July 24-27 and November 7-11, a typical number of the large space weather events per year at the peak of a solar cycle. The 5-s sampled data (i.e., sampling rate 0.2 Hz) were chosen for a better representation of the fast variations of the geomagnetic field (Trichtchenko, 2021).
Figs 5, 6 and 7 show the geomagnetic field variations of X- (i.e. North-South) component at all three stations for the entire year and during the periods of high geomagnetic activity on 3-15 November 2004.

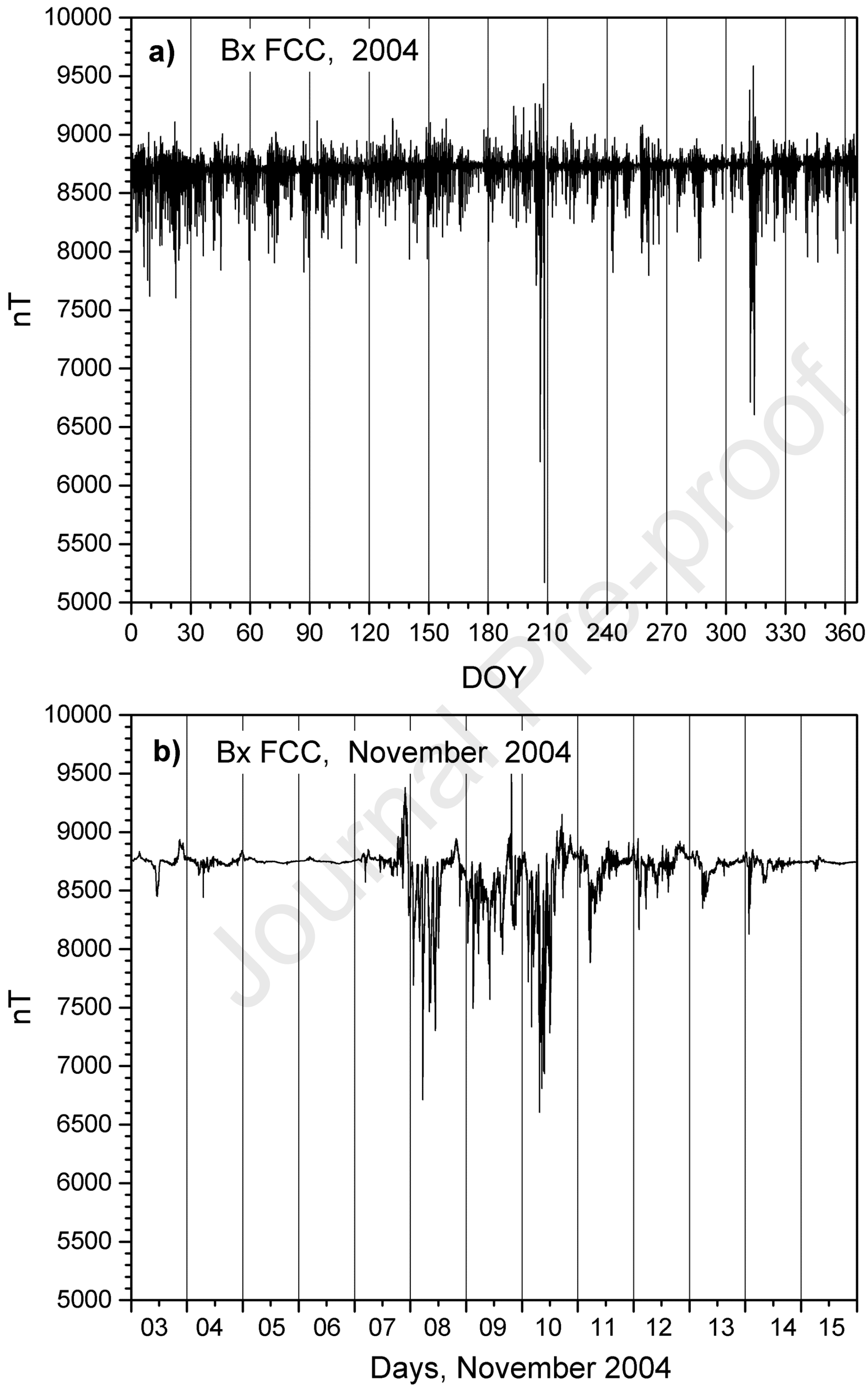


Fig. 5. Variations of X-component of geomagnetic field at FCC geomagnetic observatory during year 2004; a) the entire year b) geomagnetically active interval 3-15 November 2004.

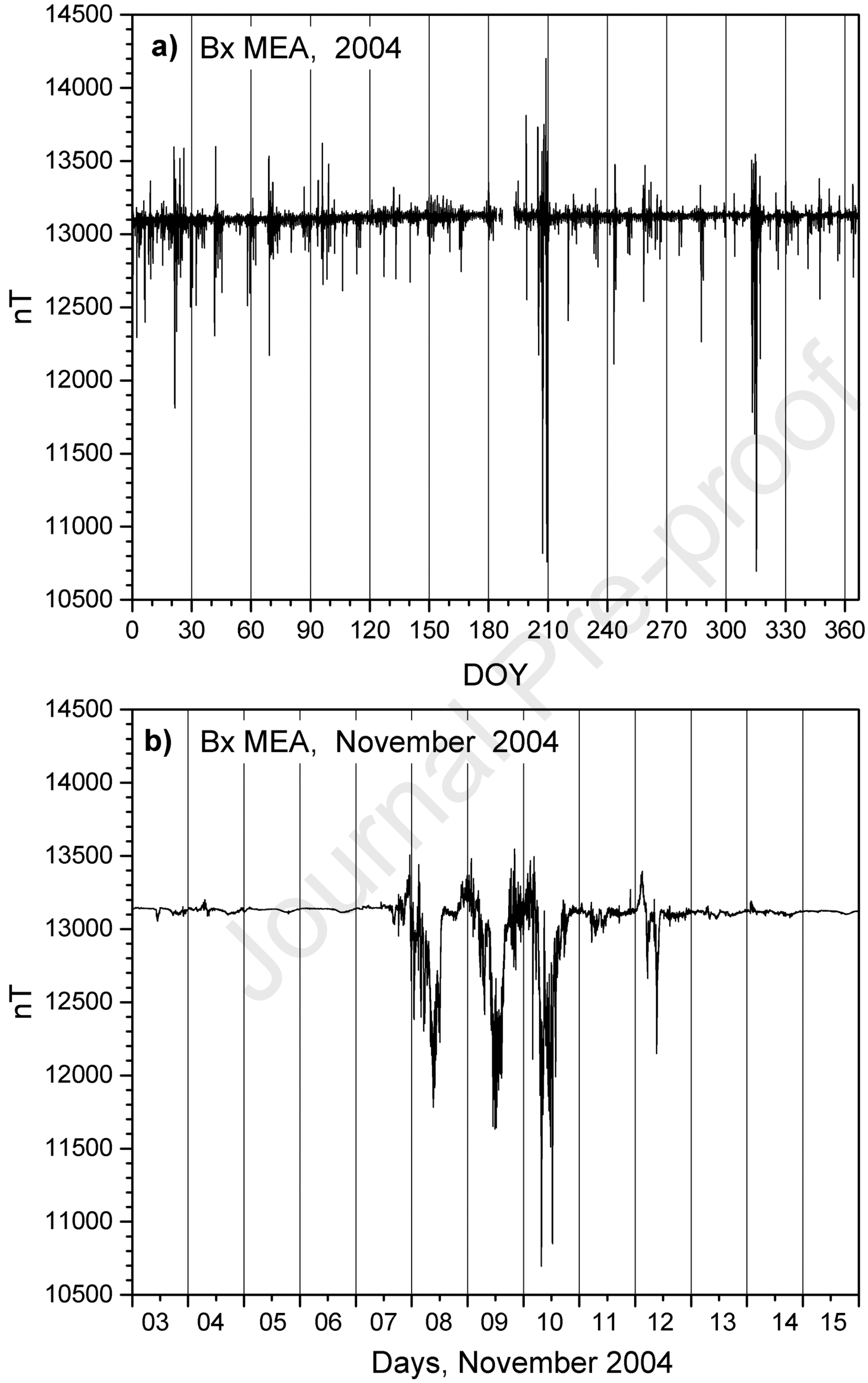


196
197 Fig. 6. The same as in Fig. 5, but for MEA geomagnetic observatory.

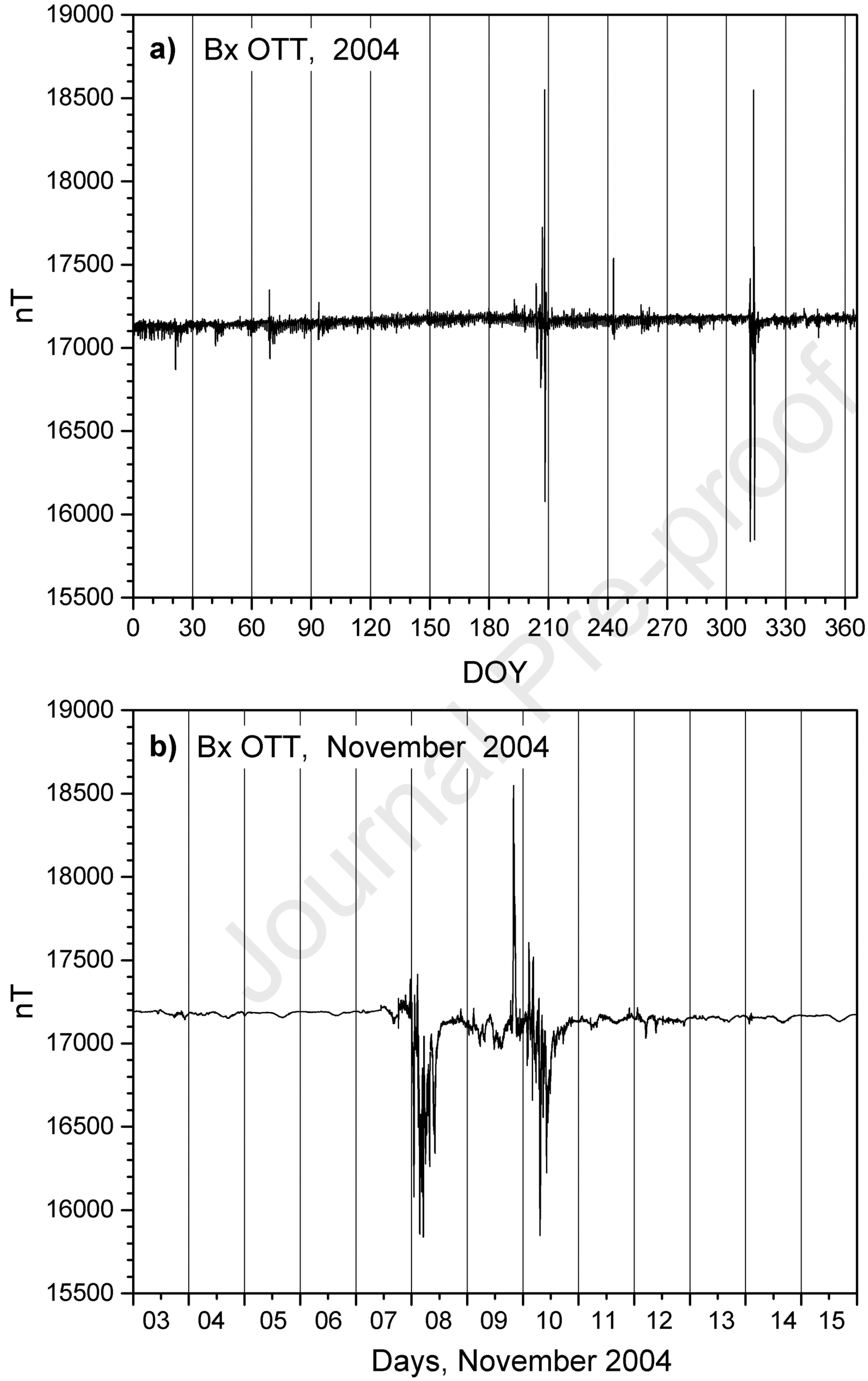


Fig. 7. The same as in Fig. 5, but for OTT geomagnetic observatory.

Comparisons of two major storm intervals in 2004, July 24-27 and November 7-10, in terms of their geomagnetic variations, show that at a high latitude FCC observatory the amplitude of the variations (~3500 nT in July and ~2150 nT in November) are much larger than at stations in lower latitudes, such as MEA (~2500 nT and ~2600 nT) and OTT (~1300 nT and ~800 nT). During November 2004 event, the increase in geomagnetic activity at all 3 stations started approximately at the same time on November 7, but continues longer at FCC (until November 14), than at MEA (until November 13) and only until November 10 at OTT. Therefore, both the amplitude and the duration of high geomagnetic activity differ significantly at all three observatories. Thus, in order to fully assess the possible impacts of geomagnetic disturbances and associated telluric currents, it is essential to include the range of representative locations.

## 3. Models used in PSP estimations

For pipeline modelling, the Distributed Source Transmission Line (DSTL) approach has been employed (Taflove and Dabkowski, 1979; Boteler, 1997; Trichtchenko and Boteler, 2002). In this approach, uniform sections of pipeline are represented by linear circuit elements with their series impedances defined by pipeline steel resistance and parallel admittances defined by coating conductance to the ground. The geoelectric field in each section is represented by voltage sources distributed along the transmission line.

Following Boteler (1997), the PSP variations (*V*) can be expressed as:

$$\frac{d^2E}{dx^2} - \gamma^2\, V = \frac{dE}{dx} \tag{1}$$

where *E* is geoelectric field along the section of pipeline (modelled with use of geomagnetic data as explained later in this Section), γ is propagation constant, defined as $\gamma = \sqrt{ZY}$ ; with *Y* is parallel admittance and *Z* is the series impedance. Although both Z and Y are generally frequency-dependent, for the frequencies of telluric variations (i.e. below 1 Hz) the inductive and capacitive parts of the pipeline impedance and admittance are negligible (Trichtchenko, 2016). As such, the series impedance can be replaced by the resistance of pipeline steel, and parallel admittance equals to the coating conductance to ground.

Solution of Equation (1) can be written as:

$$V(x) = \frac{E}{\gamma}\left(Ae^{-\gamma(x-x_1)} - Be^{-\gamma(x_2-x)}\right) \tag{2}$$

where *V(x)* is PSP variations at location *x*, and coordinates $x_1$ and $x_2$ are the positions of the pipeline ends. *A* and *B* are constants dependent on the boundary conditions at the ends of the pipeline (terminating impedances), expressed as follows:

$$A = \frac{(Z_0 - Z_c)Z_L - (Z_c + Z_L)Z_0 \exp(\gamma L)}{(Z_0 + Z_c)(Z_L + Z_c)\exp(\gamma L) - (Z_0 - Z_c)(Z_L - Z_c)\exp(-\gamma L)} \tag{3}$$

$$B = \frac{(Z_L - Z_c)Z_0 - (Z_c + Z_0)Z_0 \exp(\gamma L)}{(Z_0 + Z_c)(Z_L + Z_c)\exp(\gamma L) - (Z_0 - Z_c)(Z_L - Z_c)\exp(-\gamma L)} \tag{4}$$

where $Z_0$ and $Z_L$ are terminating impedances at both ends of pipeline (x=0 and x=L) and $Z_c$ is the pipeline characteristic impedance $Z_c = \sqrt{Z/Y}$.

The PSP variations can be calculated from Equations (1-4) when pipeline parameters and the geoelectric field are known.

The following assumptions about pipelines were made: the "hypothetical" pipeline extends in the East-West (i.e. Y-) direction with the uniform electromagnetic and geometric parameters as presented in Table 1, which corresponds to the case described in (Trichtchenko and Boteler, 2002). The PSP variations were calculated at the location point with x= 868 km, i.e. at the end of the pipeline, where the values are higher (Boteler, 1997). The East-West direction for the pipeline has been chosen to describe the extreme case, because, statistically, the geoelectric field is usually larger in this direction (Trichtchenko, 2021).

Table 1. Electrical and geometric parameters of the modelled pipeline

| Pipeline parameter | Value |
|---|---|
| Length L | 868 km |
| Pipeline series resistance Z | 0.028 Ω/km |
| Pipeline parallel admittance Y | 0.01 S/km |
| Propagation constant γ | 0.0167 $km^{-1}$ |
| Characteristic Impedance Zc | 1.67 Ω |
| Terminating Impedances $Z_0$=$Z_L$ | 0.1 Ω |
| Coating thickness c | 0.7 mm |

After substitution of values from Table 1 into Equations 2-4, the resulting PSP variations at the end of pipeline $V_L(t)$ can be expressed as:

$$V_L(t) = 3.4 \cdot E_y(t) \quad (5)$$

where $V_L$ is in mV, $E_y$ is the value of geoelectric field in mV/km.

Geoelectric field is modelled with use of the measured geomagnetic field B and the modelled surface impedance $Z_{earth}$, based on widely utilized formula presented in the magnetotelluric literature, (Simson and Bahr, 2005) as follows:

$$\left[\vec{E}\,(\omega)\right] = \frac{1}{\mu_0}\left[Z_{earth}(\omega)\right]\left[\vec{B}\,(\omega)\right] \quad (6)$$

where ω is the angular frequency, and the vectors of electric and magnetic fields are $[\vec{E}\ (\omega)] = \begin{pmatrix} Ex(\omega) \\ Ey(\omega) \end{pmatrix}$ and $[\vec{B}\ (\omega)] = \begin{pmatrix} Bx(\omega) \\ By(\omega) \end{pmatrix}$.

The components of frequency domain magnetic field are obtained with use of discrete Fast Fourier Transform (Press et al., 2007, also Trichtchenko and Boteler, 2002).

The one-dimensional Earth resistivity structure (”layered earth”) is used, i.e. the impedance Z at the top of any layer n is found by applying the recursive relation for the impedance of an N-layered half-space (Weaver, 1994).

$$Z_n = i\omega\mu_0 \left( \frac{1 - r_n exp(-2k_n l_n)}{k_n(1 + r_n exp(-2k_n l_n))} \right) \tag{7}$$

where for each layer n:

$l_n$ is the thickness,

$k_n$ is the propagation constants $k_n = \sqrt{i\omega\mu_n\sigma_n}$ ,

$\mu_n$, is relative permeability,

$\sigma_n$ is conductivity,

$r_n$ is reflection coefficient defined as:

$$r_n = \frac{1 - k_n \frac{Z_{n+1}}{i\omega\mu}}{1 + k_n \frac{Z_{n+1}}{i\omega\mu}} \ . \tag{8}$$

The impedance $Z_N$ for the last layer $N$ (uniform half-space) is $Z_N = (i\omega\mu)/k_N$ .

As the “hypothetical” pipeline extends along Y-axis, only the $E_y$ component is used for the calculations of PSP variations:

$$E_y(\omega) = -\frac{1}{\mu_0} Z_{earth}(\omega) B_x(\omega) \tag{9}$$

Conversion of the geoelectric field from the frequency domain back to the time domain has been performed with use of a discrete inverse Fast Fourier Transform (Press et al., 2007; Trichtchenko and Boteler, 2002).

Details of the layered Earth models used in the electric field calculations are presented in Appendix, Table A (after Trichtchenko et al., 2019).

## 4. Corrosion models

The theory of corrosion under steady-state conditions is based on the application of Faraday's law of electrolysis (Peabody, 2001, p.307), which states that the mass of the metal loss due to oxidation can be expressed as follows:

$$\Delta m = j \cdot a \cdot \Delta t \cdot \frac{M}{n_e \cdot F} \qquad (10)$$

where $\Delta m$ is the mass loss in grams (g), $j$ is steady-state (i.e. DC) current density in A/cm$^2$, $a$ is the exposed surface area in cm$^2$, $\Delta t$ is the time of exposure (in s), $n_e$ is the number of electrons participated in the oxidation reaction, $M$ is the molecular weight of metal, $F$ is the Faraday constant, F=96485 (Coulomb/mole). For the iron oxidation reaction, the number of electrons $n_e$=2, $M$=56 g/mole.

For practical reasons (i.e. availability of the pipe-to-soil voltage measurements), the current density $j$ in (10) is commonly replaced by voltage $V$ using von Baeckmann and Shwenk (1975, equation 38 on page 365), (also in Gummow 2002):

$$j = \frac{V}{\rho} \quad \frac{1}{\frac{\pi r}{4} + c} \qquad (11)$$

where $\rho$ is soil resistivity, $r$ is radius of coating defect, $c$ is coating thickness. Schematic geometry and example of results obtained with use of Equation (11) are presented in Fig. 8.

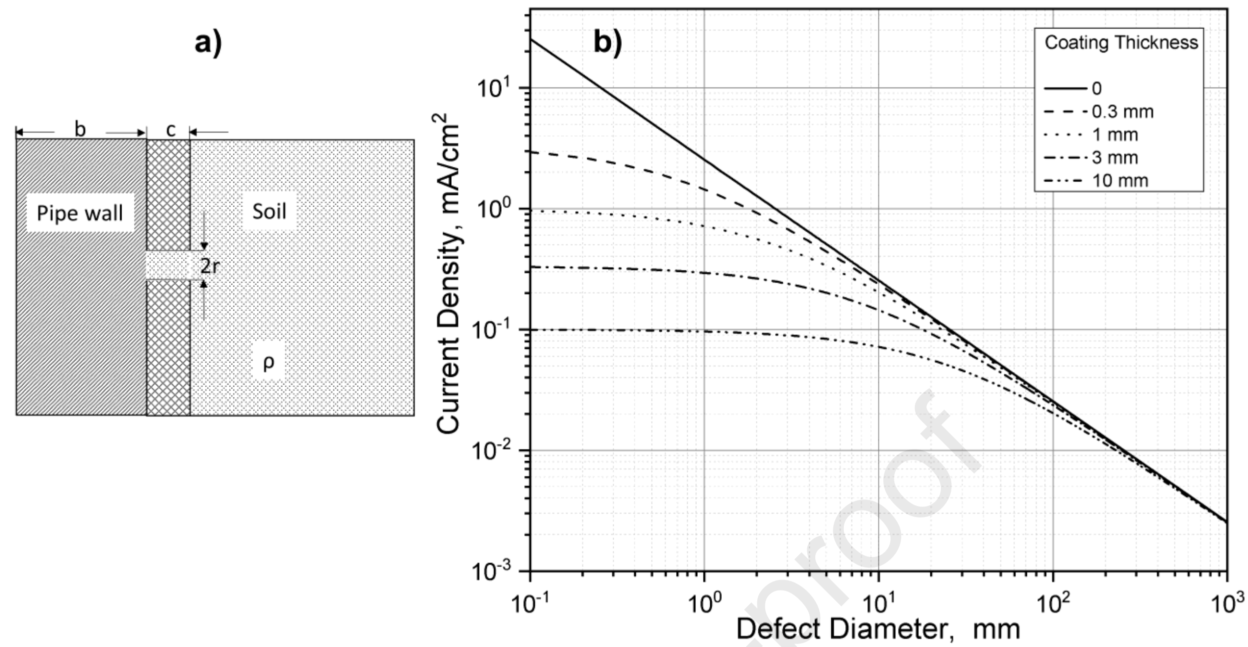


Fig. 8. a) Geometry of the coating defect (not to scale), where *b* is thickness of the pipeline wall (steel), *c* is thickness of the pipeline coating, *2r* is diameter of the coating defect; b) dependence of current density on the defect diameter for voltage drop of 1 V and soil resistivity of 1000 Ω·m for various values of coating thickness.

The mass loss is commonly expressed as $\Delta m = d \cdot a \cdot \Delta b$, where $\Delta b$ is change of the wall thickness, $d$ is iron density in g/ cm$^3$ (d=7.8 g/ cm$^3$). Substituting Equation (11) for current density and the above expression for mass loss into Equation (10), the loss of wall thickness $\Delta b$ due to DC-corrosion is expressed as:

$$\Delta b = V \cdot \Delta t \cdot \frac{M}{d n_e F} \cdot \frac{1}{\rho \cdot (\frac{\pi r}{4} + c)} \qquad (12)$$

where Δb, r, c are given in cm, voltage drop V is in V, Δt is in s, d is in g/cm$^3$; ρ is in Ω·cm Expression (12) can be rearranged in terms of DC corrosion rate ($CR_{DC}$) as:

$$CR_{DC} \left(\frac{cm}{s}\right) = \frac{\Delta b}{\Delta t} = \frac{M}{d n_e F} \frac{V}{\rho} \frac{1}{\frac{\pi r}{4} + c} \qquad (13)$$

For consistency with Gummow (2002), the defect radius has been defined as 0.5 cm and the resistivity of the host media (soil) is 1000 Ω·cm. The coating thickness *c* is 0.07 cm (Table 1). After substitution of all constants, the steady-state corrosion rate can be expressed as:

$$CR_{DC} \left(\frac{mm}{s}\right) = \frac{\Delta b}{\Delta t} = 8.0 \cdot 10^{-7} \cdot V \qquad (14)$$

where b is wall thickness in mm, t is time in s, V is anodic voltage change associated with the current flow from the pipeline through the defect in coating, in V.

The experimental results demonstrated that the corrosion rates of varying (alternating) current are reduced in comparison with DC-current (i.e. calculated with the use of Faraday's law for the same current density, geometry of the defect and soil characteristics), and this reduction depends on the period of variations (Mc Collum and Ahlborn, 1916; Qin et al, 2020; Brenna et al., 2020).

Most observations of corrosion rates are provided for periodically varying currents produced by man-made systems (i.e. power lines, trams, subways, etc.) which can enter nearby pipelines and accelerate the corrosion process. These alternating currents (AC) caused by electrical interference usually have fixed frequencies (i.e. 16.7 Hz, 50 Hz and 60 Hz and their harmonics), which are much higher than frequencies of the natural geomagnetic and telluric current variations. Telluric currents are currents produced by geomagnetic variations and have a continuous frequency spectrum in the range of $10^{-5}$ Hz to 1 Hz, corresponding to periods from 1 s to ~12 hours. The main drawback in the evaluation of telluric-related corrosion is the insufficient theoretical understanding and the absence of observations under conditions of the continuous frequency spectrum and continuously varying amplitudes of associated PSP fluctuations.

Only a very limited number of publications describe the results of experiments conducted at discrete frequencies comparable to those of the natural variations of telluric currents. In these experiments, currents with fixed periods are applied, and conditions for corrosion are created during half of the period when the current flows from the electrode (known as "anodic" exposure). After sufficient duration, the loss of metal is measured, and the corrosion rate calculated. Some details of such experiments are briefly summarized below.

- McCollum and Ahlborn (1916) presented the results of corrosion rate measurements for currents alternating at nine fixed periods, with exposure intervals from 1/60 s up to 2 weeks. The resistivity of the host media (soil) was not clearly quantified, and cathodic protection was not applied.
- Qin et al. (2020) presented the results of the experimental research on corrosion rates due to metro stray currents alternating at eleven fixed periods which correspond to the exposure intervals ranging from 5 s to 1 h. The resistivity of the host media (soil-simulated solution) was about 140 Ω·cm; no cathodic protection was applied.

- Du et al. (2021) described several types of experiments, in which corrosion rate measurements were arranged similarly to Qin et al., 2020, but expanded by the addition of a different host media (more resistive), with exposure time intervals ranging from 10 s to 16 h; no cathodic protection was applied.
- Birbilis et al. (2005) presented results of experiments dedicated to measuring corrosion rates due to telluric currents in sandy soil with a resistivity of 50,000 Ω·cm and in clay soil with a resistivity of 4,000 Ω·cm. The measurements were conducted for currents alternating with three fixed periods corresponding to exposure intervals of 1 min, 10 min and 60 min. Cathodic protection of -1 V was applied during the experiment, and voltage variations during anodic exposure were limited to 1 V (i.e. from -1 V to 0 V).

These experiments were conducted with different types of electrodes (shape, size and material), as well as host media. Different methods were applied to measure the metal loss, ranging from simple weighing (McCollum and Ahlborn, 1916) to the use of sophisticated resistance probes (corrosometers) in Birbilis et al. (2005). In all but one experiment the waveform of the applied varying currents has been described as a periodic rectangular wave, and the time of exposure equals to a half-period. The waveform of periodic current has not been clearly defined in Birbilis et al. (2005), and the time of anodic exposure in their experiment corresponded to only 20% of the fluctuation period.

The results of the experiments were presented as a ratio of the measured corrosion rate of varying current to the corresponding DC (steady-state)-corrosion rate calculated using Faraday's law (McCollum and Ahlborn, 1916; Qin et al., 2020; Du et al., 2021). The tabulated results provided in these sources were used for our modelling of telluric-associated corrosion. Because Birbilis et al. (2005) did not provide the tabulated results, the observed corrosion rates due to telluric currents and DC (steady state) corrosion rates were inferred from their graphic results.

.

Fig. 9 displays the dependence of the corrosion rate ratio on each discrete exposure time interval. It should be noted that the time of exposure is defined as the length of time interval when current flows from the pipe, i.e. transfer of electrical charge corresponds to the oxidation reaction (Peabody, 1979).

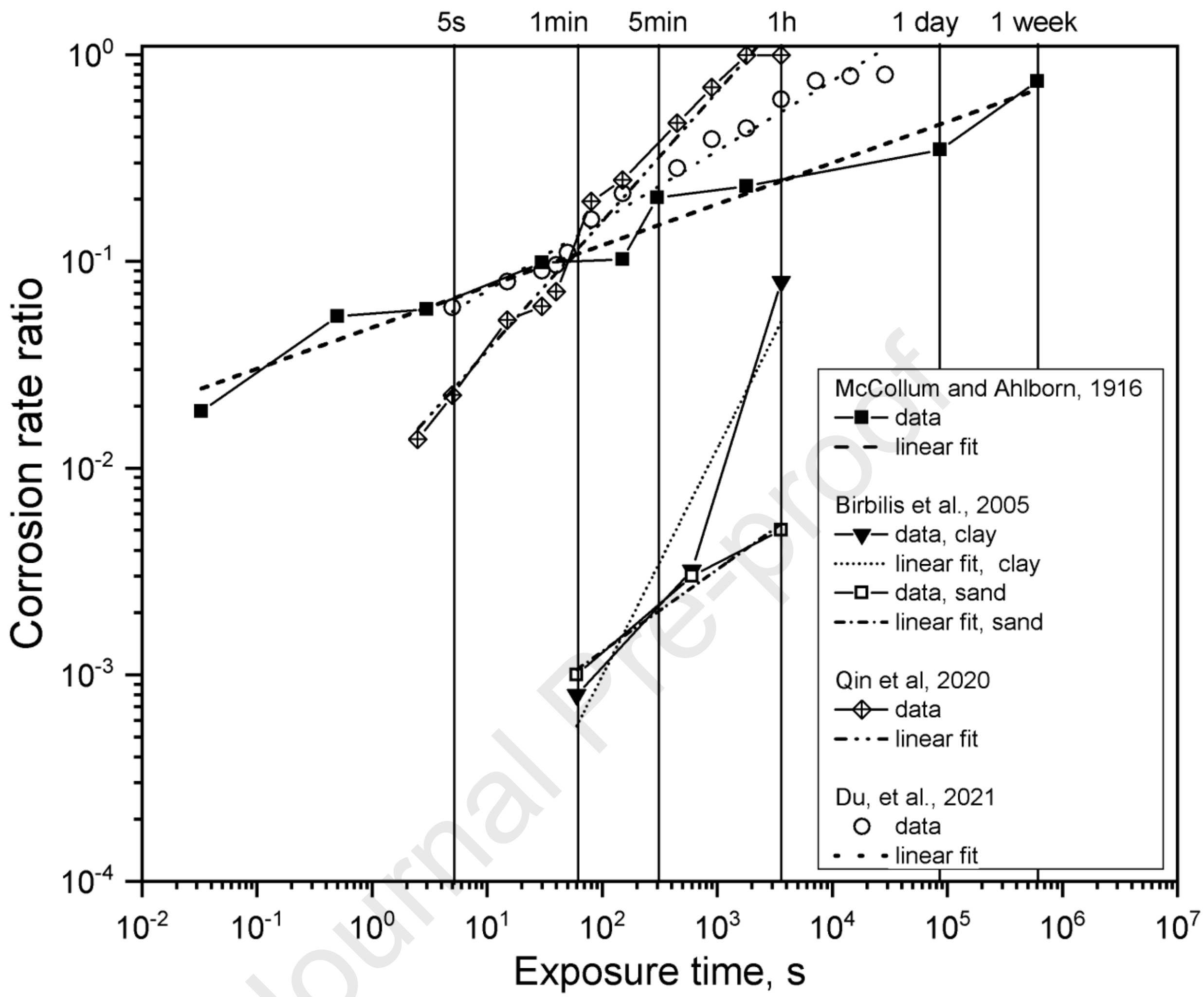


Fig. 9. Dependence of corrosion rate ratio on the exposure time intervals inferred from available publications as described in the text. References are provided in the legend. Linear fits (in logarithmic coordinates) for each dataset are shown as dashed lines. Corrosion rate ratio is the ratio of the experimentally obtained corrosion rate to the one calculated according to Faraday's law for each discrete exposure time interval.

The results of Birbilis et al. (2005) experiments yielded much smaller values compared to the other three experiments, as shown in Fig. 9. This is most likely due to the application of cathodic protection, which significantly reduces corrosion rates. For example, for the exposure time interval of 1 min, the rate reduction is almost 200 times, for the exposure time interval of 1 hour the reduction changes from 50-150 times for pipeline in sand to only 5-10 times less for pipeline in clay. However, these comparisons are not rigorous since the conditions of these experiments were not identical in many aspects.

The experiments of McCollum and Ahlborn (1916), Qin et al. (2020) and Du et al. (2021) were conducted to determine the corrosion rates caused by man-made alternating currents. Their results differ by a factor less than 5 for the most of exposure time intervals. Qin et al. (2020) estimated that the observed corrosion rate was identical to the calculated DC (steady-state)- rate for exposure time above 1 h, however, McCollum and Ahlborn (1916) concluded that this ratio was only around 75% even for the exposure time of 1 week.

According to Birbilis et al. (2005), corrosion rates in clay soils (low resistivity host media) are larger than in sandy soils (high resistivity host media) for the exposure time intervals longer than approximately 10 min. The comparison of results of Qin et al. (2020) (in less resistive host media) and Du et al. (2021) (in more resistive host media), as plotted in Fig 9, demonstrates a similar relation in corrosion rates (higher for low resistive media) for exposure time intervals longer than 1 min.

Only three out of four referenced publications were used in our analysis to evaluate the telluric-associated corrosion. The corrosion rate ratios inferred from Du et al. (2021) fell within the range of other results and, therefore, were not included.

Further analysis utilizes the following approximations of telluric-to-DC ratio of corrosion rates ($R_{cr}^{ref} = CR_{telluric}/CR_{DC}$) due to exposure of the steel to the varying telluric currents with rectangular waveform (i.e. constant current during each particular discrete exposure time interval $\Delta t_i$):

McCollum and Ahlborn (1916):

$$R_{cr}^{M\&A}(\Delta t_i) = 0.05 \cdot (\Delta t_i)^{0.2} \quad (15)$$

Qin et al. (2020):

$$\begin{gathered} R_{cr}^{Q}(\Delta t_i) = 0.0087 \cdot (\Delta t_i)^{0.63} \;\; if \; \Delta t_i < 60 \; min \\ R_{cr}^{Q}(\Delta t_i) = 1.0 \;\; if \; \Delta t_i \geq 60 \; min \end{gathered} \quad (16)$$

Birbilis et al. (2005)

$$R_{cr}^{B,sand}(\Delta t_i) = 2 \cdot 10^{-4} \cdot (\Delta t_i)^{0.4}$$
$$R_{cr}^{B,clay}(\Delta t_i) = 6 \cdot 10^{-6} \cdot (\Delta t_i)^{1.1} \; if \; \Delta t_i < 12\,h; \; R_{cr}^{B,clay}(\Delta t_i) = 1 \; if \; \Delta t_i \geq 12\,h \quad (17)$$

Taking into account the corrosion rate ratios and assuming the voltage is constant ("rectangular-wave") during each discrete interval $\Delta t_i$, Eq.(14) can be modified to calculate the telluric-associated corrosion as follows:

$$\Delta b_i\,(mm) = 8.0 \cdot 10^{-7} \cdot R_{cr}^{ref}(\Delta t_i) \cdot V_i \cdot \Delta t_i \quad (18)$$

where $R_{cr}^{ref}$ are the ratios defined by Eqs, (15)-(17), ρ is soil (host media) resistivity in Ω·cm, index *i* identifies each discrete exposure time interval ($\Delta t_i$), $V_i$ is the corresponding exposure voltage. The exposure voltage is the positive deviation of pipe-to-soil potential from the specific PSP level at which corrosion rate is negligible (CP level in our calculations). ..

The total reduction in the wall thickness over time can be calculated as the sum of losses during each interval:

$$\Delta b(mm) = 8.0 \cdot 10^{-7} \cdot \frac{1}{\rho} \sum_1^N R_{cr}^{ref}(\Delta t_i) \cdot V_i(\Delta t_i) \cdot \Delta t_i \quad (19)$$

where index *i* corresponds to each discrete exposure time interval ($\Delta t_i$), N is the total number of exposure intervals during the analyzed period (for example, during several days of November 2004 or October-November 2003 events, or during the entire year 2004).

The final expression for calculating the telluric-associated annual corrosion rate is:

$$CR_{telluric}\left(\frac{mm}{a}\right) = 25.36 \cdot \sum_1^N R_{cr}^{ref}(\Delta t_i) \cdot V_i(\Delta t_i) \cdot f_i \quad (20)$$

where $f_i$ is the length of time interval $\Delta t_i$ expressed as fraction of the year.

It should be noted that, although Faraday's law is widely used for the calculation of the corrosion rates due to alternating current (Kajiyama, 2017), the electrochemical processes at the boundary between exposed pipeline metal and the soil in the presence of cathodic protection are quite complex (Buchler, 2020; Brenna et al., 2020). Thus, formulas (19) and (20) could further be refined based on more specific theoretical and experimental results.

## 5. Results

To utilize the results of experiments conducted for "rectangular" alternating current waveforms, the recorded variations of PSP (see Figs. 3 and 4) were approximated by the sets of average values for each time interval when the PSP value reverses from being more positive/negative than the cathodic protection (CP) level, as illustrated in Fig. 10. The term "average between reversals" is used for this approximation method.

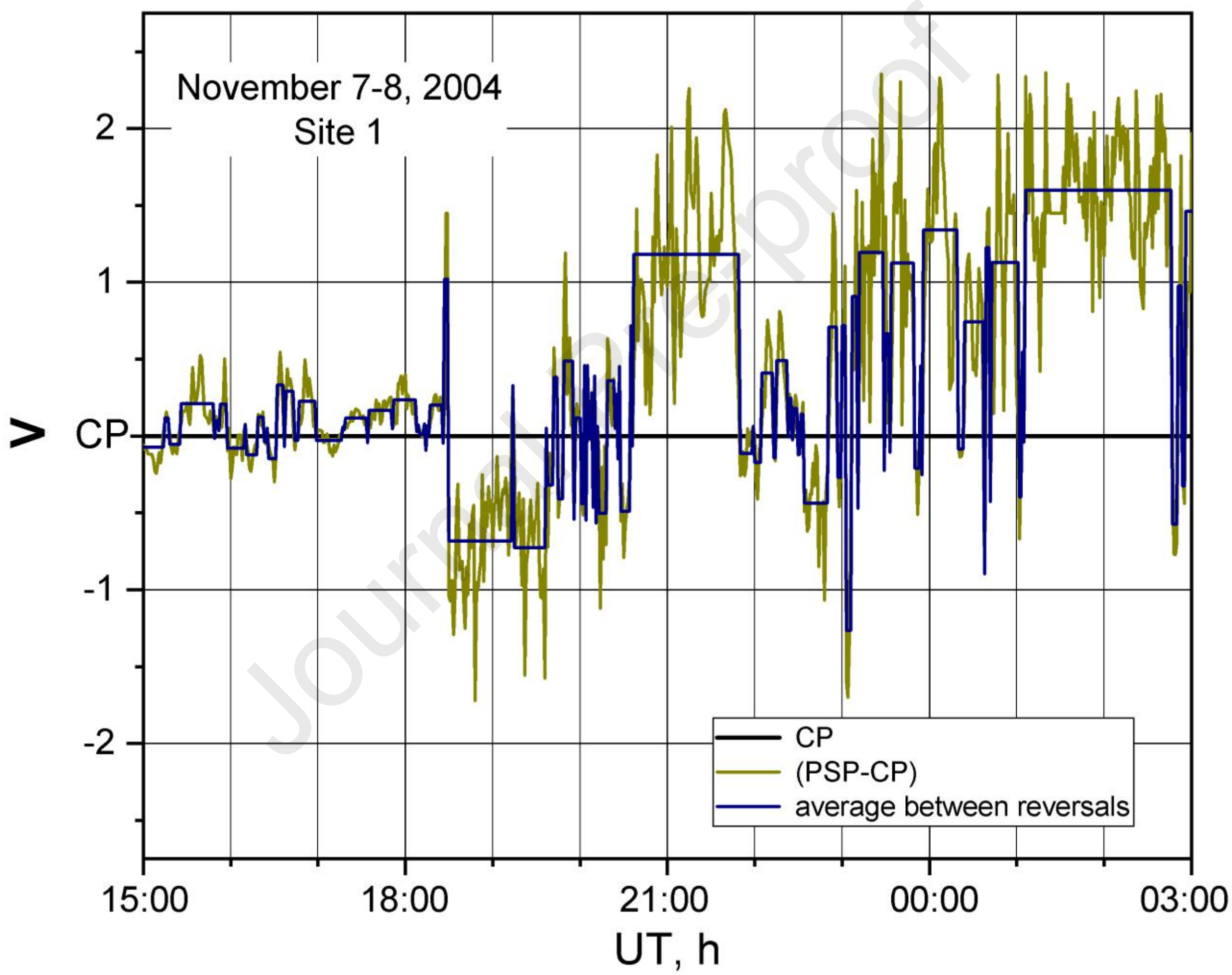


Fig. 10. Example of recorded and approximated PSP variations at Site 1 of Australian pipeline during November 7-8, 2004. Dark yellow is the original recording with the CP level subtracted (denoted as PSP-CP), blue is the average between reversals with respect to the cathodic protection level.

The steady state PSP levels without telluric interference were estimated based on PSP recordings and found to be -1.0 V±0.05 V. These values are in the range of the recommended CP values (ISO 15589-1, 2015) and are further denoted as "CP". As presented in Figs. 3,4 and 10, recorded PSP fluctuate around the CP level. The superposition of the telluric-independent PSP and telluric-associated PSP variations is discussed in Gummow, 2002.

The pipeline steel is considered protected against corrosion when the PSP equal to or more negative than the CP level is exposed to corrosion during intervals with PSP are more positive than CP level. For calculations of corrosion rates based on Equation (20), only time intervals of anodic exposure were used. This is consistent with the experiments conducted by McCollum and Ahlborn, 1916, Qin et al., 2020 and by Birbilis et al., 2005.

It should be noted that the corrosion rates based on experimental results without cathodic protection (McCollum and Ahlborn, 2016 and Qin et al., 2020) can be treated as the "worst-case scenario".

Calculated telluric-associated corrosion rates are presented in Table 2 for PSP recording on the Australian pipeline during November 3-November 15, 2004 (Fig. 3). Table 3 contains results for pipelines in the Czech Republic during the event in October-November 2003 (Fig. 4). Underlined values in Tables 2 and 3 identify the corrosion rates which exceed the recommended value 0.01 mm/year according to ISO 21857 (2021), numbers in bold are those which exceed the corrosion rate of 0.025 mm/year considered as benchmark level (NACE SP0169, 2013; Gummow, 2002).

Table 2. Loss of wall thickness (mm/year) during the November 2004 event, at different sites along the Australian pipeline. Underlined are rates above 0.01 mm/year, numbers in bold are rates above 0.025 mm/year. The ratios to the standard corrosion rates are presented in brackets, with the first number being the ratio to 0.01 mm/year, the second one to 0.025 mm/year.

| Corrosion model | Site 1 | Site 2 | Site 3 |
|---|---|---|---|
| McCollum and Ahlborn, (1916) | $2.75 \cdot 10^{-2}$<br>(2.75/1.1) | $1.68 \cdot 10^{-2}$<br>(1.68/0.7) | $\mathbf{6.10 \cdot 10^{-2}}$<br>(6.10/**2.4**) |
| Qin et al., (2020) | $\mathbf{9.58 \cdot 10^{-2}}$<br>**(**9.58/**3.8)** | $\mathbf{6.04 \cdot 10^{-2}}$<br>**(**6.04/**2.4)** | $\mathbf{2.02 \cdot 10^{-1}}$<br>(20.2/**8.0**) |

| | | | |
|---|---|---|---|
| Birbilis et al., (2005) _______sand | $5.92\cdot10^{-4}$ (0.06/0.02) | $3.34\cdot10^{-4}$ (0.03/0.01) | $1.39\cdot10^{-3}$ (0.14/0.06) |
| Birbilis et al., (2005) _______clay | $9.46\cdot10^{-3}$ (0.95/0.4) | $4.10\cdot10^{-3}$ (0.4/0.2) | $\underline{2.75\cdot10^{-2}}$ ($\underline{2.75}$/1.1) |

Table 3. Same as in Table 2, but for two sites at European pipelines during the October-November 2003 event.

| Corrosion model | Sv Katarina | Orechov |
|---|---|---|
| McCollum and Ahlborn, (1916) | $7.40\cdot10^{-3}$ (0.74/0.3) | $2.81\cdot10^{-3}$ (0.28/0.1) |
| Qin et al., (2020) | $\underline{2.10\cdot10^{-2}}$ ($\underline{2.1}$/0.8) | $1.10\cdot10^{-2}$ (1.1/0.4) |
| Birbilis et al., (2005) _______sand | $1.06\cdot10^{-4}$ (0.06/0.004) | $5.35\cdot10^{-5}$ (0.05/0.002) |
| Birbilis et al., (2005) _______clay | $4.03\cdot10^{-4}$ (0.04/0.02) | $5.30\cdot10^{-4}$ (0.05/0.02) |



As presented in Tables 2 and 3, the telluric-related corrosion rates were greater on the Australian pipeline during November 2004 event than on European pipelines during the October-November 2003 events.

The evaluation based on experimental results without cathodic protection, such as the top two rows in both tables, produces the largest estimations, i.e., the "worst-case scenario", often above the acceptable corrosion rates. These estimations lead to the following conclusions (Tables 2 and 3):
- corrosion rates based on Qin et al. (2020) were above the benchmark level of 0.025 mm/year (and, therefore, 0.01 mm/year) at all sites on the Australian pipeline.
- corrosion rates derived using McCollum and Ahlborn (1916) experimental results were above the acceptable level of 0.01 mm/year at all 3 sites on the Australian pipeline, but below the level of 0.025 mm/year only at site 3.
- corrosion rates on two sites of two European pipelines were below the level of 0.01 mm/year, and above 0.01 mm/year only at one site if estimated using Qin et al. (2020).

Corrosion rates evaluated according to Birbilis et al. (2005), i.e. with cathodic protection, led to smaller rates (bottom two rows in Tables 2 and 3), which is consistent with data presented in Fig. 9. For the Australian pipeline, the corrosion rates are below the acceptable levels for high resistivity soil (sand), while for low resistivity soils (clay) the corrosion rates can reach or exceed the level of 0.01 mm/year (at Sites 1 and 3) but stay below 0.025 mm/year. For both European pipelines, the corrosion rates estimated with CP were well below the acceptable rate of 0.01 mm/year.

Even though the PSP values during October-November 2003 event were larger on the IKL pipeline (at Sv Katarina) than during November 2004 at any site on the Australian pipeline (Figs 3 and 4), the corrosion rates at Sv Katarina were smaller than at any site on the Australian pipeline. This can be explained by the differences in the duration of the exposure intervals (i.e. intervals when PSP-CP>0), as the corrosion rates, according to Equation (20), depend not only on the voltage levels but also on the duration for each voltage level.
To analyze this effect, the "average between reversals" exposure voltages (i.e. difference between PSP and CP during exposure intervals) are plotted versus their corresponding durations in Fig. 11 and Fig. 12.

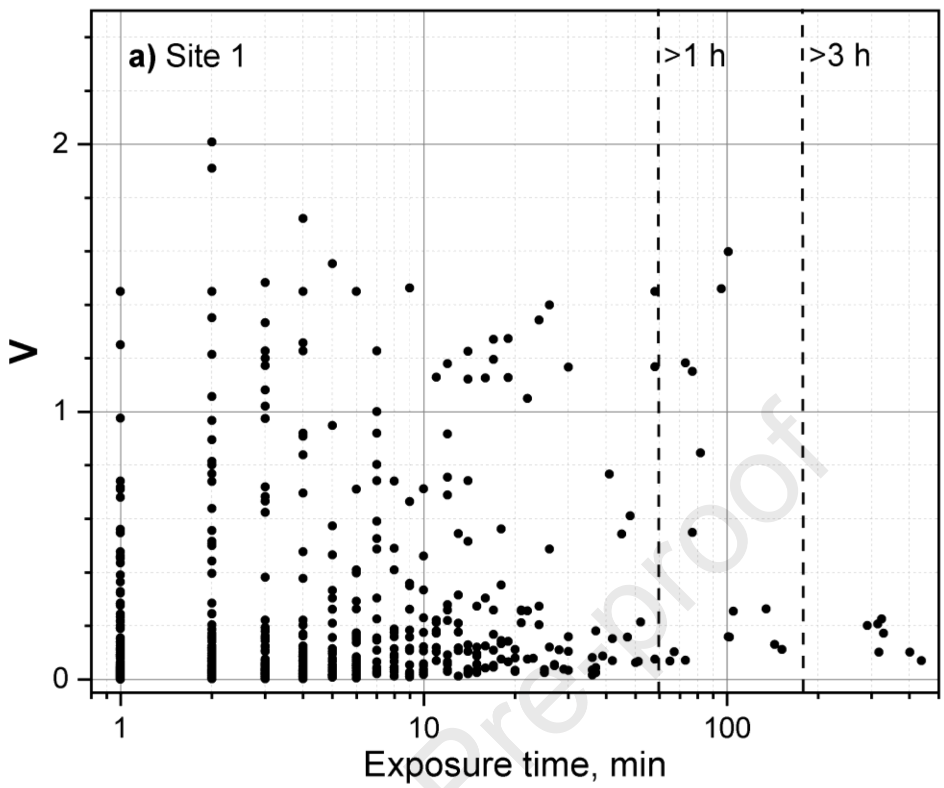
a) Site 1
>1 h
>3 h
V
0
1
2
1
10
100
Exposure time, min

a)

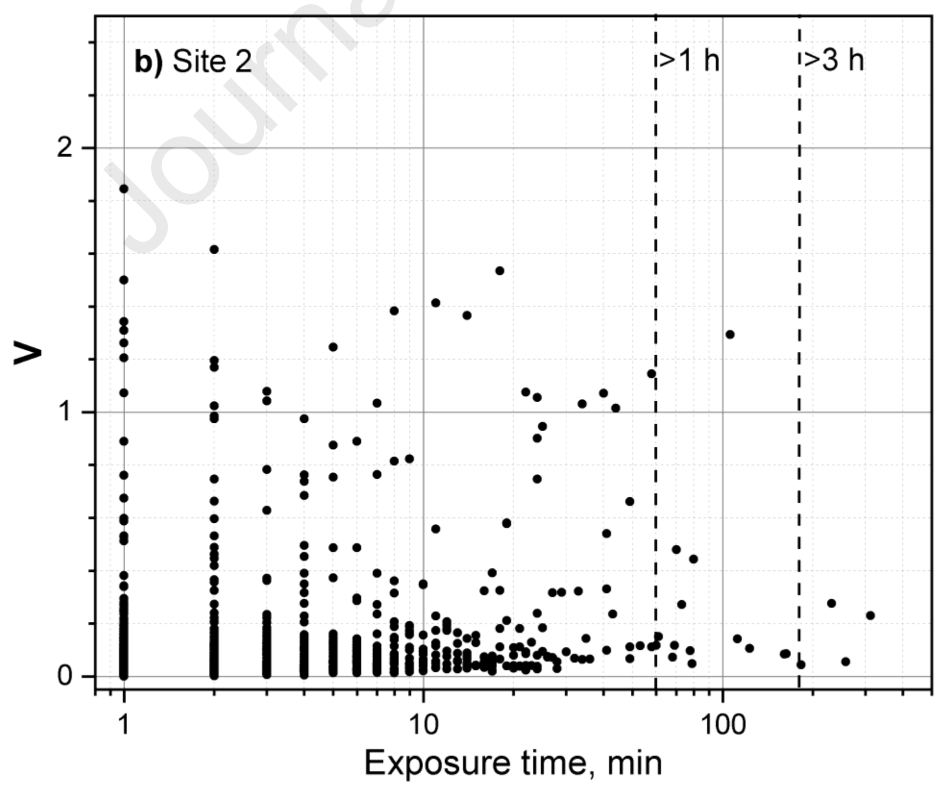
b) Site 2
>1 h
>3 h
V
0
1
2
1
10
100
Exposure time, min

b)

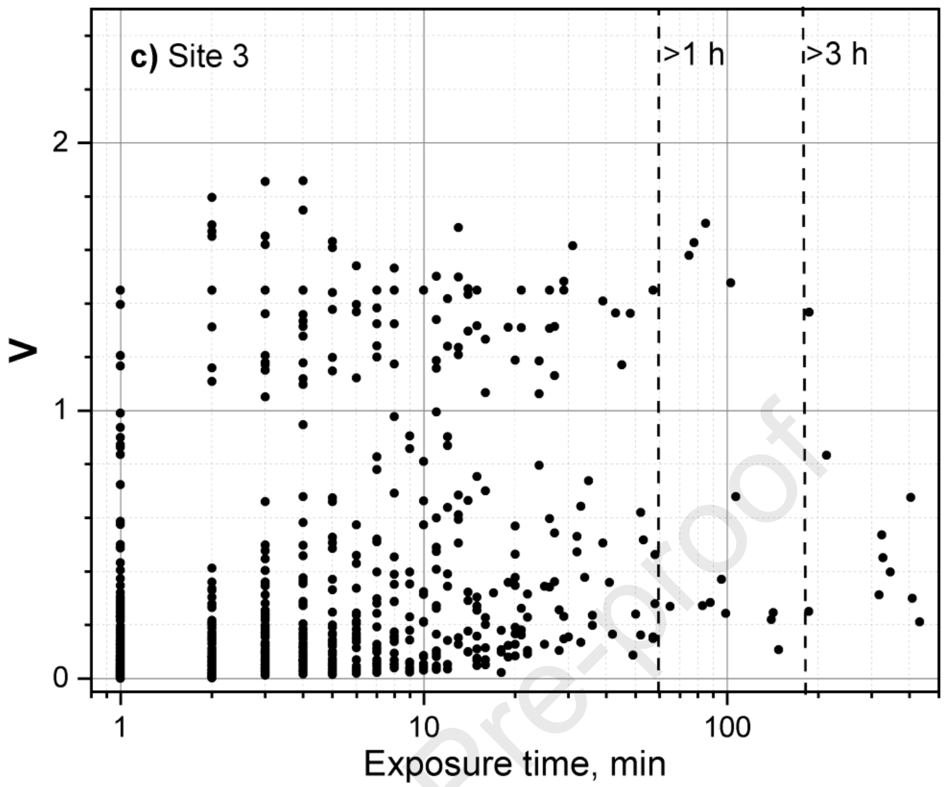


c)

Fig. 11. The “average between reversals” exposure voltages (i.e. positive PSP-CP values) versus corresponding duration of exposure intervals for each Australian pipeline measurement site: a) Site 1; b) Site 2; c) Site 3.

At Site 1 (Fig. 11a) and Site 2 (Fig. 11b) the (PSP-CP) values were smaller for longer intervals (>1h and >3 h) than those at Site 3 (Fig. 11 c). The data for Site 3 included significantly more cases with large (PSP-CP) values during longer exposure intervals. There were several cases where (PSP-CP) values reached 1.8 V and lasted longer than 1 h and when (PSP-CP) value ~ 1.4 V lasted longer than 3 h. Because the corrosion rate is directly proportional to the duration of exposure and corresponding voltage (Eq. 20), the corrosion rate at Site 3 was the largest among all three sites on the Australian pipeline.

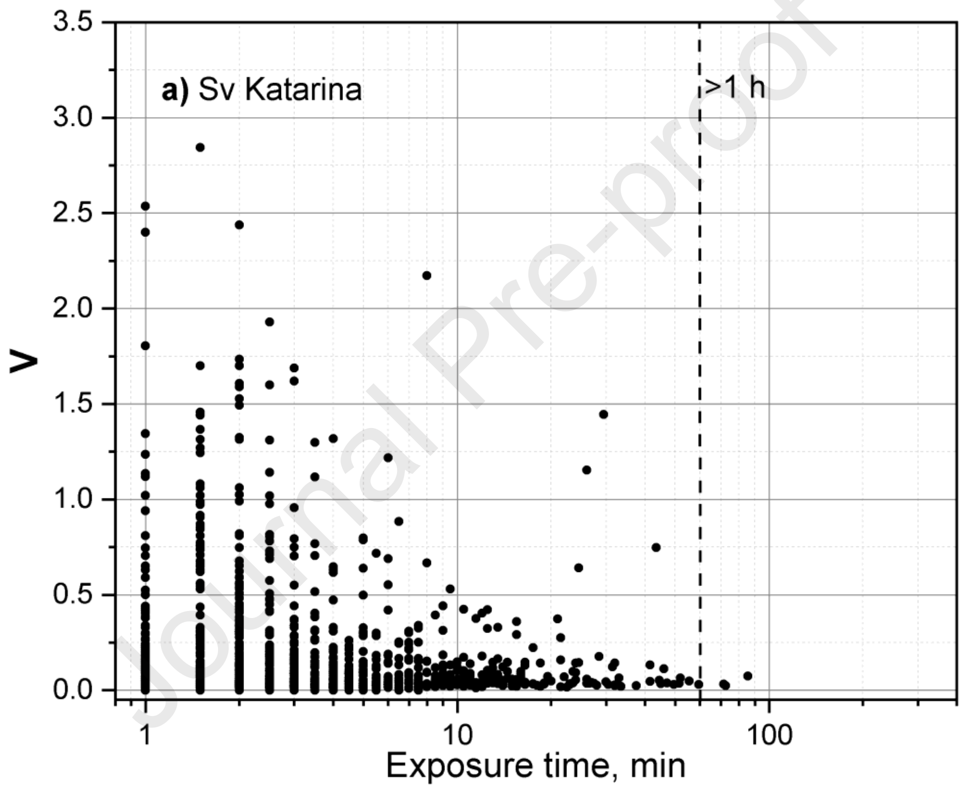


a)

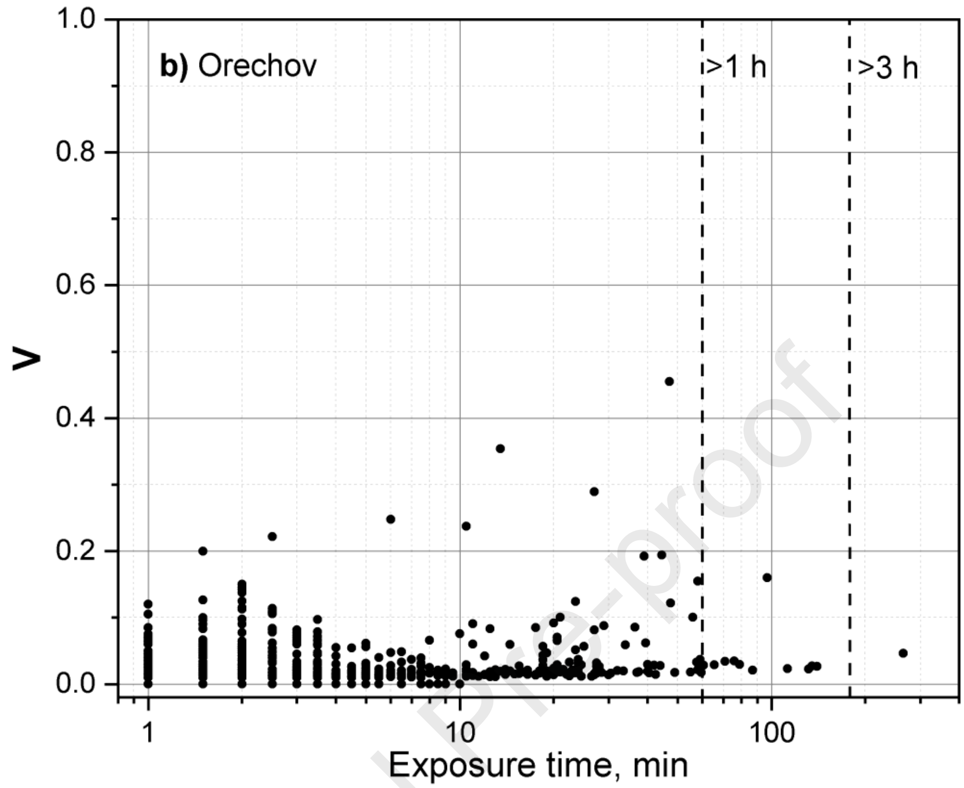


b)

Fig. 12. The same as in Fig. 11, but for October-November 2003 event and pipelines in Europe: a) at Sv Katarina site (IKL pipeline) and b) at Orechov site (Druzba pipeline).

The large exposure voltages (3.9 V) at Sv Katerina, as shown in Fig. 12a for October 2003-November 2003 event, correspond to exposure time of less than 10 min and in many cases even less than 3 min, while long-lasting exposures were typically characterized by a very small PSP-CP<0.25 V. The exposure time intervals longer than three hours were not detected. Thus, the smaller corrosion rate on the European pipeline, located at mid-latitudes, than on the near-equatorial Australian pipeline was due to the dominance of the shorter exposure intervals between voltage reversals.

There were several exposure intervals with a duration longer than 1 h at Orechov (Fig. 12b), but they did not lead to significant corrosion rates due to their relatively small amplitude (see also Table 3).

It should be noted, that, while corrosion rates obtained in experiments without cathodic protection represent the "worst-case scenario", the application of results based on Birbilis et al. (2005) can underestimate the corrosion rates. They have pointed out, that the exposure time in their experimental procedure has been limited to the time when voltage changed between -1 V (CP level) and 0 V only. In reality, there are many cases when the telluric-associated PSP values are greater than 0 V (as shown in Figs. 3 and 4), which would inevitably increase the corrosion rates in comparison with the ones obtained in their experiment.

The evaluation of the corrosion rates for modelled PSP time series at three locations with different geomagnetic activity has been conducted in a similar way. Telluric variations of PSP are directly proportional to the geoelectric field (Equation 5), which, in turn, is obtained with application of the forward and backward Fourier transform. As a result, fluctuations of telluric-associated PSP around zero are obtained, because this method does not account for any DC-offset. A constant CP level can be added to the modelled voltage fluctuations to obtain the total PSP variations around CP level. The example of modelled PSP and the "interval-average"-approximation is presented in Fig. 13 for the period of geomagnetic disturbance observed on November 8, 2004 (OTT location).

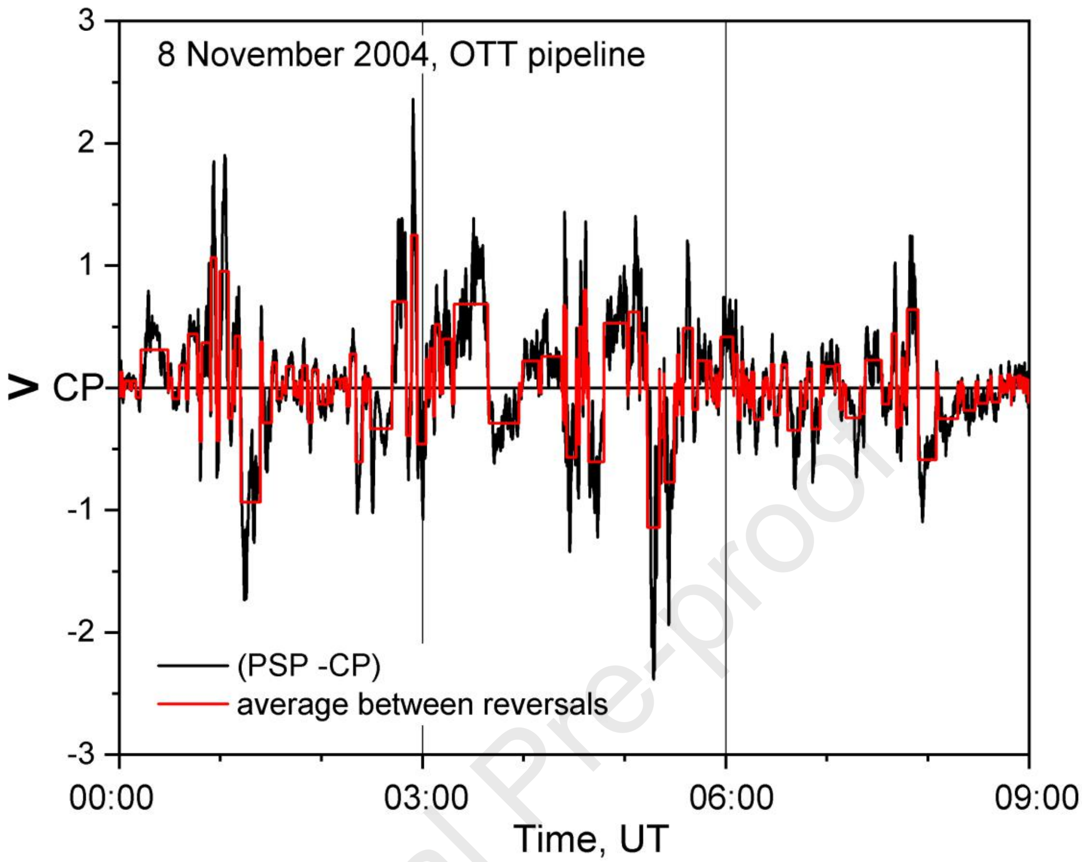


Fig. 13. Example of modelled telluric-associated PSP variations (5-s sampling interval) and "average between-reversals" approximation for the "hypothetical" pipeline located near OTT magnetic observatory during 15 most active hours on November 7-8, 2004. Black line is modelled PSP, red line is the average between reversals.

Estimates of the telluric-associated corrosion rates for the entire year 2004 based on modelled telluric-associated PSP time series for 3 different locations (OTT, MEA, and FCC) are presented in Table 4. Underlined values are those exceeding the annual corrosion rate of 0.01 mm/year (ISO 21857, 2021), and values in bold are values exceeding 0.025 mm/year (NACE SP0169 (2013); Gummow (2002).

Table 4. Loss of pipeline wall thickness (mm/year) for three locations of the modelled pipeline. Underlined are rates above 0.01 mm/year and numbers in bold are rates above 0.025 mm/year.

The ratios to the acceptable corrosion rates are presented in brackets, with the first number being the ratio to 0.01 mm/year, and the second is the ratio to 0.025 mm/year.

| Corrosion model | OTT (45.4°N) | MEA (54.6°N) | FCC (58.8°N) |
|---|---|---|---|
| McCollum and Ahlborn, (1916) | $1.66{\cdot}10^{-2}$ (1.66/0.7) | **$8.18{\cdot}10^{-2}$** (8.2/**3.3**) | **$1.25{\cdot}10^{-1}$** (12.5/**5.0**) |
| Qin et al., (2020) | **$4.20{\cdot}10^{-2}$** (4.2/**1.7**) | **$1.92{\cdot}10^{-1}$** (19.2/**7.7**) | **$2.42{\cdot}10^{-1}$** (24.2/**9.7**) |
| Birbilis et al., (2005) sand | $2.27{\cdot}10^{-4}$ (0.02/0.01) | $1.08{\cdot}10^{-3}$ (0.11/0.04) | $1.50{\cdot}10^{-3}$ (0.15/0.06) |
| Birbilis et al., (2005) clay | $7.58{\cdot}10^{-4}$ (0.07/0.03) | $2.77\ 10^{-3}$ (0.27/0.1) | $2.80{\cdot}10^{-3}$ (0.28/0.1) |

The largest corrosion rates are obtained using experimental results without cathodic protection applied. Among them, results based on Qin et al., (2020) for any pipeline location, and based on McCollum and Ahlborn (1916) for two locations (MEA and FCC) were significantly above the level of 0.025 mm/year.

The telluric-associated corrosion rates for "hypothetical" pipelines based on Birbilis et al. (2005) with cathodic protection applied, are well below the acceptable rates. However, these results can underestimate the corrosion rates because, as noted earlier, the experiment has been limited to a potential change of 1 V, thus defining the "lower envelop" for evaluation of telluric-associated corrosion.

In terms of the pipeline location, the largest telluric-associated corrosion rates were obtained for the auroral zone (FCC), which has the highest level of geomagnetic activity (Fig. 5). The lowest rates were in the sub-auroral zone (OTT), a location with the lowest geomagnetic activity among all three stations (Fig. 7). The results for a pipeline near MEA were at the intermediate level, which is consistent with the geomagnetic activity at MEA (Fig. 6).

The distribution of "average between reversals" exposure voltages versus the corresponding duration of exposure time intervals are plotted in Fig. 14 a-c for three different zones of geomagnetic activity in order to analyse the joint effect of exposure duration and magnitude.

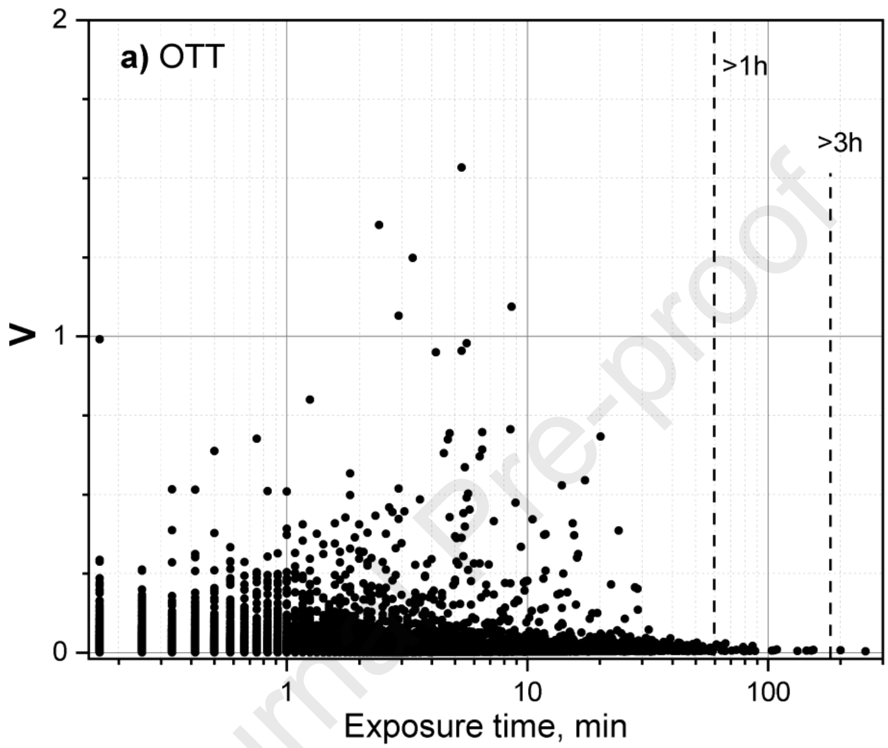


a)

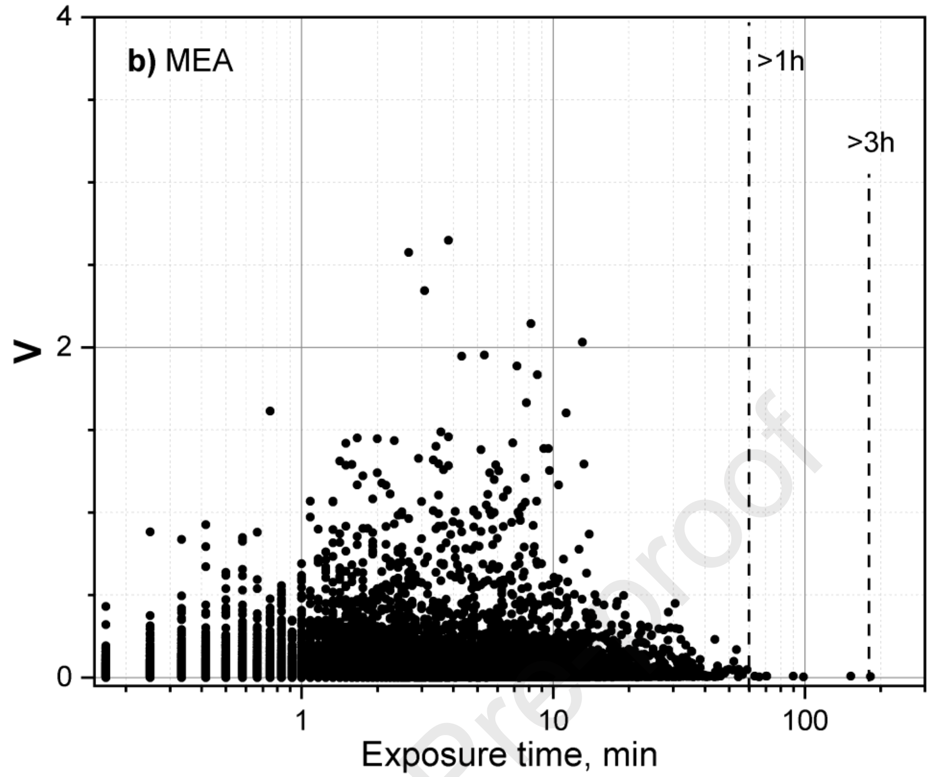
b) MEA
>1h
>3h
V
0
2
4
1
10
100
Exposure time, min

b)

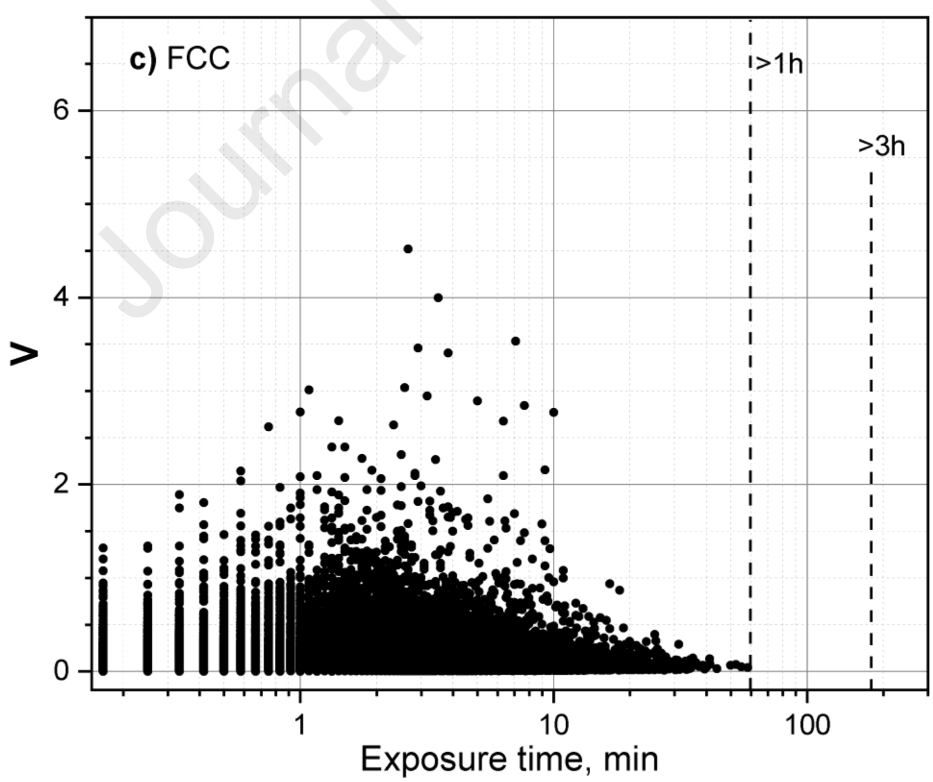
c) FCC
>1h
>3h
V
0
2
4
6
1
10
100
Exposure time, min

c)

Fig. 14. The “average between reversals” exposure voltages versus the corresponding duration of exposure time intervals for modelled pipeline during the year 2004 at three locations. a) OTT (latitude 45.4°N), b) MEA (latitude 54.6°N) and c) FCC (latitude 58.8° N).

The comparison of Figs. 14 a -c shows that the largest telluric-associated voltages of about 4.5 V are obtained from FCC geomagnetic data, followed by MEA (2.75 V) and OTT (1.5 V). This is consistent with the geomagnetic activity levels at these latitudes. The modelled telluric-associated PSP variations at OTT (45.4°N, Fig. 14a) are comparable with the recordedexposure voltages at Sv Katarina (~50°N, Fig.12a) despite possible differences in the pipelines' characteristics. It provides some additional confidence in the modelled telluric-associated PSP variations.

The exposure time intervals between 1 min and 15 min corresponded to the largest “average between reversals” exposure voltages for modelled PSP (Fig. 14a-c). As for the observed exposure voltages (Figs. 11 and 12), the largest values corresponded to exposure time intervals between 2 min to 2 h (Australian pipeline), 2 min-10 min (IKL) and 20-30 min (Druzba). The shorter durations of the exposure time intervals for modelled PSP explain relatively small corrosion rates for modelled variations in comparison to the recorded data.

The two cases with exposure interval above 3 hours (albeit very small average voltage values) occurred only at the OTT location (Fig. 14 a). The exposure intervals above 1 h occurred several times at OTT and MEA locations (Fig. 14 a and b) and there are no such long exposure intervals at higher latitude (FCC, Fig. 14 c). This can be explained by the differences in the nature of the geomagnetic variations. While in the sub-auroral zone (OTT) the largest geomagnetic variations are associated with the slow variations (main phase and recovery phase of the geomagnetic storms), which comprise several hours in duration, the geomagnetic activity within the auroral zone (MEA, and especially at FCC) is mainly associated with faster variations, produced by the mix of high-speed solar wind and geomagnetic substorms.

The latitudinal dependence of normalized (to OTT) telluric-associated corrosion rates at three locations calculated using four experimental corrosion models is plotted in Fig. 15.

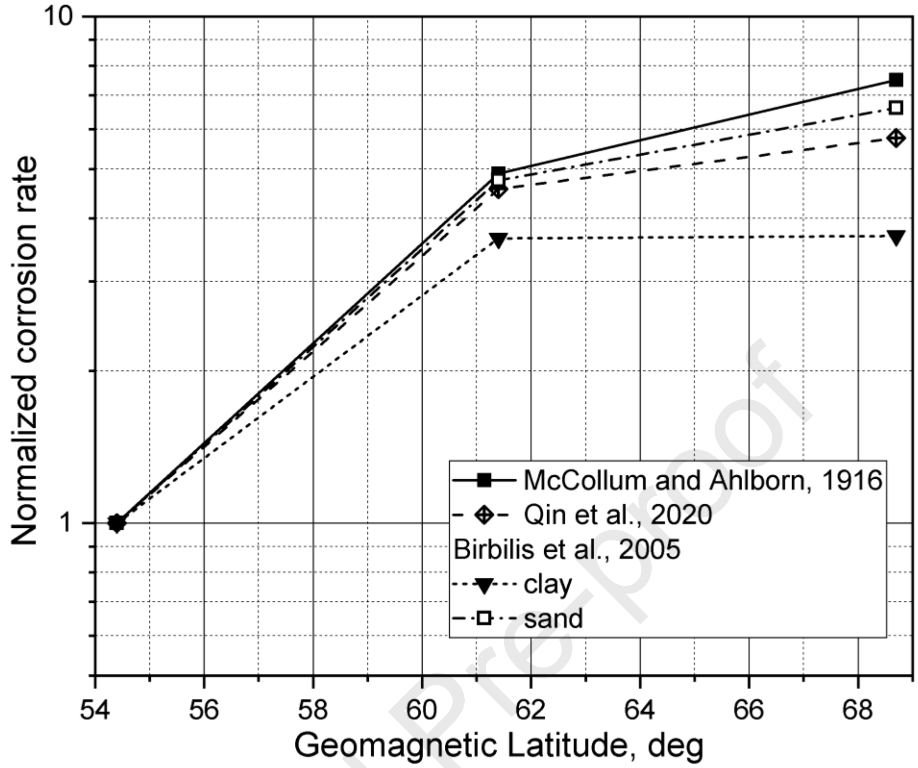


Fig. 15. Dependence of annual telluric-associated corrosion rates on geomagnetic latitude calculated using four published experimental results, as described in the legend. The values are normalized to the corrosion rate for the OTT pipeline. Telluric-associated PSP variations were modelled for the year 2004.

The increase in the corrosion rates with latitude is significant (factor of 3.5 to 4.5) for the transition from subauroral (OTT) to auroral (MEA) zones. It is significantly less pronounced (1. to 1.5) within the auroral oval, i.e. for the transition from MEA to FCC. The geomagnetic coordinates and locations of the observatories with respect to the auroral zone were identified according to Fiori et al. (2020). Regardless of the utilized experimental results (i.e. obtained with or without CP), the telluric-associated pipeline corrosion is higher at the auroral latitudes for the same pipeline characteristics.

## 6. Discussion

The response of pipelines to the geomagnetic activity in terms of PSP variations and currents along the pipeline has been observed and modelled in many studies (Campbell, 1980; Boteler and Seager, 1998; Pulkkinen et al., 2001; Viljanen et al., 2010; Marshall et al., 2010; Ingham et al., 2022; see also an extended list of references in Boteler and Trichtchenko, 2015). However, estimations of the possible increase in corrosion due to slow varying telluric currents (with periods from 1s to~12 hours) did not attract similar attention, and very limited attempts to quantify this effect have been made. Some researchers utilized the DC-corrosion approximation (Faraday's law of electrolysis) and reported contrasting conclusions, e.g., the effect of telluric-related corrosion in Gideon et al. (1970) was quantified as negligible, while in Osella et al. (1998, 1999) it is estimated as an important factor leading to the reduction of pipeline lifetime. The results of the old experimental study by McCollum and Ahlborn (1916) on the corrosion rates of alternating currents for a wide range of fixed reversal periods show that corrosion rates decrease with a decrease in reversal periods and are smaller than DC (steady state) corrosion rates even after a week of exposure.

These results were later brought to the attention of the scientific community by Campbell (1978) and Peabody (1979) who concluded that the impacts of varying telluric currents on pipeline corrosion are small but require further investigation, especially for northern pipelines where significant geomagnetic variations could continue for a long time.

At the turn of the century, Gummow (2001, 2002) published new results with the analysis of increased corrosion due to telluric activity and concluded that corrosion due to telluric currents can be significant on the cathodically-unprotected pipelines. Several recent papers include estimations of corrosion rates based on Gummow's publications, such as Ingham and Rodger, 2018; Khanal et al., 2019; Moraes et al., 2020. All of the above studies on telluric-associated corrosion used the results of the experiments published by McCollum and Ahlborn (1916), obtained without the application of cathodic protection.

Our evaluation of telluric-associated corrosion extends the approach presented in Gummow (2002) and utilizes several recently published results on measurements of AC corrosion rates beyond McCollum and Ahlborn (1916), such as Birbilis et al. (2005), Qin et al. (2020) and Du et al. (2021). Among them, only in experiments by Birbilis et al. (2005) were cathodically protected electrodes used, and the lowest corrosion rates, up to 100 times smaller than in the other three references, were obtained. The main reasons of for such differences could result from the application of cathodic protection, as well as differences in the other parameters such as soil resistivity, etc.

Results from the experiments without cathodic protection also differ from each other quite significantly. For example, McCollum and Ahlborn (1916) obtained the largest corrosion rates for exposure times from 2 s to 1 min. while Qin et al. (2020) provided the largest rates for exposure time >1 min. The results of McCollum and Ahlborn (1916) did not reach the maximum (DC) level even for exposure time exceeding 1 week, while the results of Qin et al. (2020) reached the upper limit for the exposure time of 1 hour. Thus, the conditions of experiments and utilized procedures can make a significant impact on results.

The spread in experimental results leads to an expanded range of our estimates of telluric-associated corrosion, as presented in Tables 2-3 for observed PSP variations at different pipelines and in Table 4 for modelled PSP variations during one year on the identical “hypothetical” pipeline at several locations.

The obtained high corrosion rates, which exceed the benchmark level of 0.025 mm/year are associated with the application of the results of Qin et al. (2020) and McCollum and Ahlborn (1916) experiments without cathodic protection. These “upper envelop” estimations, can be regarded as the “worst-case scenario”.

The application of results from Birbilis et al. (2005) (measurements with CP) led to significantly lower estimates. These estimates exceeded the acceptable level of 0.01 mm/year only in one case considered in our study (for the pipeline in clay). However, caution should be exercised when considering these low levels. . As pointed out by Birbilis et al. (2005), underestimation is expected in their experiments because voltage variations were limited to change between -1 V and 0 V only, while fluctuations of larger amplitude often occur, as presented in Figs. 3 and 4.

Our analysis shows that, despite the fact that geomagnetic variations are lower near the equator than at other latitudes, the telluric-associated corrosion can be higher on the near-equatorial pipeline (e.g. in Australia) than that for mid-latitudes location (in Europe). A sizable response of near-equatorial and low-latitude pipelines to geomagnetic activity was observed and presented in Barker and Skinner (1980), Ogunade (1986), Marshall et al. (2010), Ingham and Rodger (2018). Measurements performed on a pipeline in Australia by Martin (1993) reported corrosion rates of up to 0.038 mm/year. We obtained similar values ranging between 0.0275 and 0.061 mm/year as presented in Table 2.

The situations when pipelines located at lower latitudes are exposed to higher corrosion rates than those located at higher latitudes emphasize the importance of considering not only the amplitude and duration of geomagnetic fluctuations, but also pipeline characteristics (such as coating, type of metal, geometric parameters, and topology) in estimation of the telluric-associated corrosion. Presented formulas for calculations of the corrosion rates can be applied to a wide range of conditions and parameters. The developed approach can be adjusted in the future when the effects of the duration of exposure and its amplitude on electrochemical processes at the interface of cathodically protected pipeline and soil during telluric-associated variations are better understood.

## 7. Summary

This paper presents an evaluation of telluric-associated corrosion for two scenarios:

- observed pipe-to-soil (PSP) variations during geomagnetic storms;
- modelled PSP variations over one year for locations with different geomagnetic activity.

The derived formulas incorporate exposure intervals of varying durations and amplitudes and are flexible regarding the selection of the threshold potential (assumed as CP level in our calculations) and other relevant parameters.

To evaluate the corrosion rates due to the telluric currents with the continuous frequency spectrum, published results of corrosion rates obtained at fixed frequencies of variations were utilized. These observational studies varied significantly in their experimental setups and procedures, which impacted the obtained estimates of telluric corrosion rates.

The evaluations based on the experimental results obtained without cathodic protection are significantly higher than acceptable corrosion rates of 0.01 mm/year (ISO 21857, 2021) and even 0.025 mm/year (NACE SP 0169:2016). These estimations should be regarded as the “worst-case scenario” for possible telluric-associated corrosion.

The evaluations based on the utilization of experimental data obtained with cathodic protection exceeded the acceptable level of 0.01 mm/year only at one location on the Australian pipeline. It has been pointed out by the authors (Birbilis et al., 2005), that these results most likely underestimate the real situation, as the utilized experimental data were obtained by limiting the voltage variations to within 1V.

The analysis of observed PSP time series demonstrated that telluric-associated corrosion rates can be higher on near-equatorial pipelines than on pipelines located at higher latitudes due to the differences in the pipeline structural parameters and operational and environmental (soil) characteristics.

Analysis of the modelled PSP variations on the identical “hypothetical” pipeline located at different latitudes demonstrated the increase of telluric-associated corrosion rates with latitude by factor of 5 when the location changes from subauroral to auroral latitudes.

Further detailed experimental and theoretical investigations specifically dedicated to telluric-associated corrosion are required to better account for a continuous spectrum and varying amplitudes of telluric current associated with geomagnetic activity.

**Acknowledgements**

The authors would like to thank the staff of the Geomagnetic Laboratory, Natural Resources Canada, and especially Dr. David Boteler for the fruitful discussions and helpful suggestions. The authors are thankful to pipeline companies for sharing their proprietary data for this research. We sincerely appreciate all valuable comments and suggestions provided by the reviewer, which helped us in improving the quality of the manuscript.

Geomagnetic data used in this paper are available from https://www.geomag.nrcan.gc.ca/index-en.php and on request from nrcan.geomagnetic-info-info-geomagnetic.rncan@canada.ca .

PSP measurements were provided by private companies with restrictions on their use and sharing.

Natural Resources Canada Contribution number 20220171.

805 **Appendix**

806

807 Table A. Parameters of the layered Earth models used with magnetic data for each observatory.

| **FCC** | | **MEA** | | **OTT** | |
|---|---|---|---|---|---|
| Thickness (m) | Conductivity (S/m) | Thickness (m) | Conductivity (S/m) | Thickness (m) | Conductivity (S/m) |
| 40 | 0.033 | 65 | 0.02 | 26 | 0.02 |
| 550· | 0.01 | 2700 | 0.067 | 900 | 0.004 |
| 16000 | $1.1 \cdot 10^{-4}$ | 9000 | 0.0003 | 9100 | 0.0002 |
| 13000 | $6.9 \cdot 10^{-5}$ | 17000 | 0.0004 | 15000 | 0.01 |
| 10000 | $1.2 \cdot 10^{-4}$ | 10000 | 0.0005 | 15000 | 0.005 |
| 61000 | 0.002 | 61000 | 0.001 | 61000 | 0.004 |
| $15 \cdot 10^4$ | 0.0063 | $15 \cdot 10^4$ | 0.0063 | $10 \cdot 10^4$ | 0.0063 |
| $16 \cdot 10^4$ | 0.035 | $16 \cdot 10^4$ | 0.02 | $16 \cdot 10^4$ | 0.035 |
| $11 \cdot 10^4$ | 0.125 | $11 \cdot 10^4$ | 0.05 | $11 \cdot 10^4$ | 0.125 |
| $15 \cdot 10^4$ | 0.42 | $15 \cdot 10^4$ | 0.18 | $15 \cdot 10^4$ | 0.42 |
| $23 \cdot 10^4$ | 0.89 | $23 \cdot 10^4$ | 0.63 | $23 \cdot 10^4$ | 0.89 |
| $10 \cdot 10^4$ | 2.08 | $10 \cdot 10^4$ | 0.89 | $10 \cdot 10^4$ | 2.08 |

808

809

## References

Barker, R. H., Skiner, N.J., 1980. The flow of electric currents of telluric origin in a long metal pipeline and their effect in relation to corrosion control, 1980, Mater Performance, Vol. 19, No.2, pp.25-28.

Birbilis, N., Holloway, L.J., Forsyth, M., 2005. Simulated transient loss of cathodic protection for buried pipelines, NACE International, Corrosion, Vol. 61, No. 5, pp. 498-501.

Boteler, D.H., 1997. Distributed-source transmission line theory for electromagnetic induction studies, Proc. 1997 Zurich EMC Symposium, Feb. 18-20, URSI supplement, 401-408, ETH, Zurich, 1997

Boteler, D. H., Seager, W. H., 1998. Telluric currents: A meeting of theory and observations, Corrosion, 54, pp.751–755.

Boteler, D.H., Trihtchenko, L., 2015. Telluric influence on pipelines, in: Revie R. W. (ed.), Oil and Gas Pipelines: Integrity and Safety Handbook, J. Wiley & Sons, Inc., Hoboken, NJ.

Brenna, A.; Beretta, S.; Ormellese, M., 2020. AC Corrosion of Carbon Steel under Cathodic Protection Condition: Assessment, Criteria and Mechanism. A Review. Materials 2020, 13, 2158. https://doi.org/10.3390/ma13092158

Buhler, M., 2020, On the Mechanism of Cathodic Protection and Its Implications on Criteria Including AC and DC Interference Conditions, Corrosion, https/doi: 10.5006/3379

Campbell, W. H., 1978. Induction of auroral zone electric currents within the Alaska pipeline, Pageoph., V 116, pp.1143-1173.

Campbell, W. H., 1980. Observation of electric current in the Alaska oil pipeline resulting from auroral electrojet current sources, Geophys J Roy Astr S, 61(2), 437-449. https://doi.org/10.1111/j.1365-246X.1980.tb04325.x.

Degerstedt, R.M., Kennelley, K.J., Lara, P.F., Moghissi, O.C. 1995. Acquiring "Telluric-nulled" Pipe-to-soil Potentials on the Trans Alaska pipeline, NACE International Corrosion ’95, Paper No. 345, pp.1-26.

Du, Y., Qin, H., Liu J., Tang, D., 2021. Research on corrosion rate assessment of buried pipelines under dynamic metro stray current, Mater Corros, 72:1038–1050. https://doi:10.1002/maco.202012082

Gideon, D.N., Hopper, A.T., Thompson, R.E., 1970. Earth current effects on buried pipelines; analysis of observations of telluric gradients and their effects, American Gas Association., cat no L30570, 77 pp.

Gummow, R.A., 2001. Telluric current effects on corrosion and corrosion control systems on pipelines in cold climate, Proceedings NACE North West Area Conference, Ancorage, Alaska.

Gummow, R.A., 2002. GIC effects on pipeline corrosion and corrosion protection systems. J Atmos Sol-Terr Phy, 64, 1755-1764.

Hejda, P., Bochníček, J., 2005. Geomagnetically induced pipe-to-soil voltages in the Czech oil pipelines during October-November 2003, Ann. Geophys., 23, 3089–3093. https://doi.org/10.5194/angeo-23-3089-2005

Ingham, M., Rodger, C. J., 2018.Telluric field variations as drivers of variations in cathodic protection potential on a natural gas pipeline in New Zealand. Space Weather, 16, 1396–1409. https://doi.org/10.1029/2018SW001985

Ingham, M., Divett, T., Rodger, C. J., Sigley, M., 2022. Impacts of GIC on the New Zealand gas pipeline network. Space Weather, 20, e2022SW003298. https://doi.org/10.1029/2022SW003298

ISO 13623, 2017. Petroleum and natural gas industries - Pipeline transportation systems. ISO – International Organization for Standardization; Geneva, Switzerland.

ISO 15589-1, 2015, Petroleum, petrochemical and natural gas industries - Cathodic protection of pipeline systems - Part 1: On-land pipelines. ISO - International Organization for Standardization; Geneva, Switzerland.

ISO 18086, 2019. Corrosion of Metals and Alloys. Determination of AC Corrosion. Protection Criteria. ISO - International Organization for Standardization; Geneva, Switzerland.

ISO 21857, 2021. Petroleum, petrochemical and natural gas industries – Prevention of corrosion on pipeline systems influenced by stray currents. ISO - International Organization for Standardization; Geneva, Switzerland.

Kajiyama, F., 2017. Risk assessment of fluctuating stray current interference on buried steel pipelines with cathodic protection applied, Proceedings, CEOCOR, 2017, Luxembourg.

Khanal, K., Adhikari, B., Chapagain, N. P., Bhattarai, B., 2019. HILDCAA-related GIC and possible corrosion hazard in underground pipelines: A comparison based on wavelet transform. Space Weather, 17, 238–251. https://doi.org/10.1029/2018SW001879

Marshall, R. A., Waters, C. L., Sciffer, D., 2010. Spectral analysis of pipe to soil potentials with variations of the Earth's magnetic field in the Australian region. Space Weather, 8, S05002. https://doi.org/10.1029/2009SW000553

Martin, B.A., 1993. Telluric Effects on a buried pipeline, Corrosion, 49(4), pp. 343-350

McCollum, B., Ahlborn, G.H., 1916. Influence of frequency of alternating or infrequently reversing current on electrolytic corrosion. National Bureau of Standards Tech Paper No 72, 1916.

Moraes, J. F., I. Paulino, L. R. Alves, C. M. Denardini., 2020. Evaluation of possible corrosion enhancement due to telluric currents: case study of the Bolivia–Brazil pipeline, Ann. Geophys., 38, 881–888, 2020. https://doi.org/10.5194/angeo-38-881-2020

NACE SP0169, 2013, Item No. 21001. Control of External Corrosion on Underground or Submerged Metallic Piping Systems.

NACE TM0497, 2018. Measurement Techniques Related to Criteria for Cathodic Protection on Underground or Submerged Metallic Piping Systems.

NACE SP0104, 2020. Techniques for Monitoring and Measuring Corrosion and Related Parameters in Field Applications.

Ogunade S. O., 1986. Induced electromagnetic fields in oil pipelines under electrojet current sources, in Phys Earth planet in, 43, pp. 307-315.

Osella, A., Favetto, A., Lopez, E., 1998. Currents induced by geomagnetic storms on buried pipelines as a cause of corrosion. J Appl Geophys, 38(3), 219–233.

Osella, A., Favetto, A., Lopez, E., 1999. Corrosion rates of buried pipelines caused by geomagnetic storms, Corrosion, 55 (7), 699-705.

Peabody, A. W., 1979. Corrosion aspects of arctic pipelines. Mater. Performance, 30, 27–32.

Peabody, A. W., 2001. Peabody's Control of pipeline corrosion, 2nd ed., NACE International, NACE Press, Houston, TX 77084.

Place, T D, Sneath, T O, 2001, Practical telluric compensation for pipeline close-interval surveys Materials Performance; 40, 9; Materials Science & Engineering Collection p. 22

Press, W. H., Teukolsky, S. A., Vetterling, W. T., Flannery, B. P., 2007. Numerical Recipes: The Art of Scientific Computing, Third Edition ,1256 pp. Cambridge University Press, ISBN-10: 0521880688.

Pulkkinen, A., Viljanen, A., Pajunpää, K., Pirjola, R., 2001. Recordings and occurrence of geomagnetically induced currents in the Finnish natural gas pipeline network. J. Appl. Geophys., 48(4), 219–231.

Qin, H., Du, Y., Lu, M., Meng, Q., 2020. Effect of dynamic DC stray current on corrosion behavior of X70 steel. Mater Corros, Volume71, Issue 1, pp. 35-53, January 2020. https://doi.org/10.1002/maco.201911022

Revie R. W. (ed.), 2015. Oil and Gas Pipelines: Integrity and Safety Handbook, J. Wiley & Sons, Inc., Hoboken, NJ.

Roberge P., 2008. Corrosion Engineering: Principles and Practice, New York, McGraw-Hill

Seager, W.H., 1991. Adverse telluric effects on Northern pipelines, in: International Arctic Technology Conference, Ancorage, Alaska, SPE22178, May 1991, p.7.

Taflove, A., Dabkowski, J., 1979. Prediction method for buried pipeline voltages due to 60 Hz AC inductive coupling, IEEE T Power Ap. Syst., vol PAS-98, 780–794.

Trichtchenko, L., Boteler, D.H., 2002. Modelling of geomagnetic induction in pipelines, Ann. Geophys., 20, 1063–1072. https://doi.org/10.5194/angeo-20-1063-2002 .

Trichtchenko, L., Zhukov, A., van der Linden, R., Stankov, S. M., Jakowski, N., StanisJawska, I., Juchnikowski, G., Wilkinson, P., Patterson, G., Thomson, A. W. P., 2007. November 2004 space weather events: Real-time observations and forecasts, Space Weather, 5, S06001. https://doi:10.1029/2006SW000281

Trichtchenko, L., 2016. Modelling natural electromagnetic interference in man-made conductors for space weather applications. Ann. Geophys. vol. 34, issue 4, 2016 p. 427-436. https://doi.org/10.5194/angeo-34-427-2016

Trichtchenko, L; Fernberg, P A; Boteler, D H., 2019. One-dimensional layered Earth models of Canada for GIC applications, part 1: General description. Geological Survey of Canada, Open File 8594, 2019, 66 pages. https://doi.org/10.4095/314804

Trichtchenko, L., 2021. Frequency considerations in GIC applications. Space Weather vol. 19, issue 8, p. 1-26. https://doi.org/10.1029/2020SW002694 .

Viljanen, A., Koistinen A., Pajunpää,K., Pirjola, R., Posio P., Pulkkinen A., 2010. Recordings of Geomagnetically Induced Currents in the Finnishnatural gas pipeline - Summary of an 11-year period, Geophysica, 46(1–2), 59–67.

Von Baeckmann, W., Schwenk, W., 1975. Handbook of Cathodic Protection, Portcullis Press, England, p. 365.

Highlights:

- Telluric-associated corrosion can exceed the maximum safe rate of 0.025 mm/a;
- It depends on the properties of pipeline and geomagnetic activity;
- Telluric-related corrosion demonstrate the latitudinal dependence;
- On specific pipelines, corrosion can be high at low latitudes;

**Declaration of interests**

☒ The authors declare that they have no known competing financial interests or personal relationships that could have appeared to influence the work reported in this paper.

☐ The authors declare the following financial interests/personal relationships which may be considered as potential competing interests: